In the following document are reported a point-by-point reply to the comments of the reviewers, along with the first submitted version of the paper and the revised one due to the comments received.

We applied all the modification as explained in the replies to the referees, although some of them were placed in different points of the paper in order for it to be more readable. Moreover, the boundaries of the directional sectors and the considered return periods have been further changed in order to get more robust results.

The parts removed are underlined in red, whereas the new ones are underlined in blue.

Nat. Hazards Earth Syst. Sci. Discuss., https://doi.org/10.5194/nhess-2018-113
Manuscript under review for journal Nat. Hazards Earth Syst. Sci.
Discussion started: 7 May 2018

Natural Hazards and Earth System Sciences
Discussions

Coastal vulnerability assessment: through regional to local downscaling of wave characteristics along the Bay of Lalzit (Albania)

Francesco De Leo[1], Giovanni Besio[1], Guido Zolezzi[2], and Marco Bezzi[2]

[1]Dept. of Civil, Chemical and Environmental Engineering - University of Genoa, Genoa, 16145, Italy
[2]UNESCO Chair in Engineering for Human and Sustainable Development - Dept. of Civil, Environmental and Mechanical Engineering - University of Trento, Trento, 38123, Italy

Correspondence to: Francesco De Leo (francesco.deleo@edu.unige.it)

Abstract.

Coastal vulnerability is evaluated against inundation risk triggered by waves run-up, through the employment of coastal vulnerability indexes (referred to as "CVI") introduced by Bosom García and Jiménez Quintana (2011). CVI are assessed through different wave climate characterizations, referring to regional (offshore wave climate) or local (near-shore wave climate) scale. The study is set along the Lalzit Bay, a coastal area nearby Durrës (Albania). The analysis reveals that the results vary due to uncertainties inherent in the run-up estimation, showing that the computational procedure should be developed by taking into account detailed information about local wave climate, especially concerning seasonal behaviour and fluctuations. Different approaches in choosing wave characteristics for run-up estimation affect significantly the estimate of shoreline vulnerability. The analysis also shows the feasibility and challenges of applying CVI estimates in contexts characterized by limited data availability, through targeted field measurements of the coast geomorphology and an overall understanding of the recent coastal dynamics and related controlling factors.

1 Introduction

Coastal zones are often characterized by a fragile equilibrium, being subjected to hydro-geomorphic processes that change their shape over time and space, and are as well under stress due to the presence of conflicting human activities (Kamphuis, 2010). Moreover, these areas have a huge socio-economic value, which has often triggered their high exploitation in the last decades: coastal population is constantly increasing, together with maritime commerce and coastal tourism (Neumann et al., 2015). This implies enhanced anthropogenic pressures, which challenge their sustainable management and preservation.

The present paper focuses on extreme natural storm events and on their impact on coastal vulnerability within such complex framework. As clearly specified by the Integrated Protocol on Coastal Zone Management ("ICZM"), the effect of storms should be embedded into coastal zone territorial plans and policies, yielding coastal vulnerability assessment (UNEP, 2008). Efficient assessment and decision support tools are required, providing easily accessible information for decision-makers.

Coastal Vulnerability Indexes represent a viable assessment option, because they are helpful to classify the shorelines in relation to their vulnerability towards extreme events, such as storms induced inundation and erosion.

These indexes usually take into account the long term wave statistics and the geomorphology of the beaches to evaluate the level of risk they are exposed to. The estimate of the environmental risk, coupled with the evaluation of the existing anthropic pressure (economic and industrial activities) leads to vulnerability maps. Different approaches to compute CVI have been so far proposed, which differently combine environmental and socio-economic relevant variables (Soukissian et al., 2010; Di Paola et al., 2014; Fitton et al., 2016; Satta et al., 2016; Armaroli and Duo, 2017; Ciccarelli et al., 2017; Óscar Ferreira et al., 2017; Ferreira Silva et al., 2017; Montreuil et al., 2017; Narra et al., 2017; Mavromatidi et al., 2018, among others). A methodological issue of particular concern is related to the computation of wave climate characteristics suitable for calculating values of the CVI that are of management significance. This can be illustrated by referring to the practical procedure proposed by Bosom García and Jiménez Quintana (2011), to assess coastal vulnerability to inundation. The procedure foresees to compute the long term run-up values, starting from the ones evaluated through the model of Stockdon et al. (2006), and then combining it with the berm or dune heights of a shore to achieve its run-up vulnerability. However, Stockdon et al. (2006) formulation intrinsically leads to a very conservative result, as it provides a value linked to the 2% probability of exceedance: this means that, for given wave and beach characteristics, the computed run-up is not the one most likely occurring, but one of the highest possibly observed within a hypothetical series of records. Therefore, evaluation of high return period run-up values could lead to highly overestimated coastal vulnerability, as the return period is closely tied to the probability of non exceedance. Conversely, the model of Stockdon et al. (2006) has shown to provide more reliable run-up estimates if the input wave parameters are provided in the near-shore region at a depth of 10 m, instead of referring to deep-water values as the original formulation suggests (Sancho-García et al., 2012). This requires to change the scale of the wave climate characterization, moving from a national/regional scale to a more detailed local scale in order to obtain reliable estimates for coastal inundation. Such downscaling of the risk analysis implies that wave conditions have to be first propagated towards the shore to evaluate shallow water parameters and afterwards to compute run-up accordingly, leading to more reliable run-up *expected value* estimate in the case of extreme events (Di Risio et al., 2017).

The main goal of the present paper is to quantify differences in assessing coastal vulnerability to inundation when using a regional and a local (near-shore) characterization of the wave climate, and in consideration of its seasonality. The study refers to the bay of Lalzit, immediately north of the city of Durrës (Albania, see Fig. 1). The focus on such rapidly developing context also allows to discuss the potential implications of coastal vulnerability assessment when decision-making requires to be highly adaptive and when data availability is scarce. Preliminary studies on the characteristic wave climate characterized its seasonal directional frames. Building such information, it has been possible to compute seasonal vulnerability indexes to be then compared with the offshore omni-directional ones. Such seasonal risk approach is particularly relevant because it could highlight the critical issues related to coastal zone management when the littoral use and exploitation change drastically between different seasons, and represents an additional novelty of the present work.

CVI assessment was performed through the Bosom García and Jiménez Quintana (2011) procedure, referring both to offshore and near-shore wave data, to evaluate variations in shoreline vulnerability depending on the employed spatial (regional/local) and temporal scale (extreme events/seasonal/directional).

The paper is organized as follows: in Sect. 2 we present the indexes computation procedure, along with the investigation area and the data used; in Sect. 3 we show results of coastal vulnerability using wave dataset at regional and near-shore scales; in Sect. 4, results are presented and possible future developments and improvements are discussed.

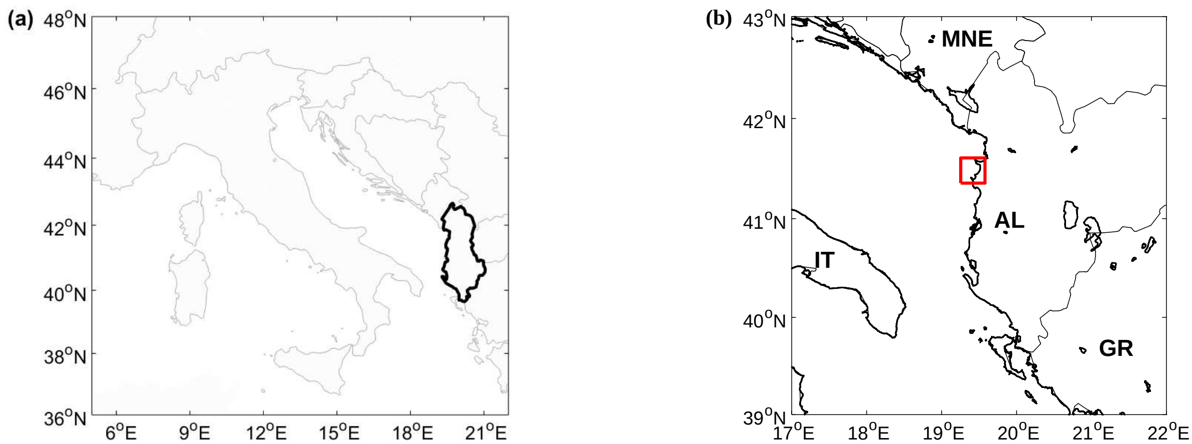

Figure 1. Map showing the area under investigation. A) Location of Albania in South-East Europe and B) the bay of Lalzit underlined within the red frame

2 Data & Methods

The vulnerability assessment is part of a wider research project, aimed at evaluating and quantifying the ongoing coastal erosion affecting the Lalzit bay area. This phenomenon is due to different causes, concerning the abrupt changes occurred in Albania after the fall of the communist regime that triggered very fast morphological changes either in the watersheds and on the coast (De Leo et al., 2017). In order to collect all the required data, a two weeks field campaign was performed during the month of July 2015.

2.1 Study area: Lalzit Bay, Albania

The Lalzit Bay is included between two capes, and can therefore be considered as an independent physiographic unit; it is possible to focus on the processes affecting this coastline independently from those characterizing the nearby physiographic units. A physiographic unit is indeed defined as a portion of shoreline with coherent characteristics in terms of natural coastal processes and of land use, which can thus be studied independently from neighbouring shores (UNEP, 2008). Specifically, in

Nat. Hazards Earth Syst. Sci. Discuss., https://doi.org/10.5194/nhess-2018-113
Manuscript under review for journal Nat. Hazards Earth Syst. Sci.
Discussion started: 7 May 2018

Natural Hazards and Earth System Sciences
Open Access
Discussions

the Lalzit bay area we identified four main interdependent geophysical and anthropogenic processes that control the dynamics and evolution of the coastal zone (see Fig. 2). The strong interaction among such processes has been identified by De Leo et al. (2017) as the main mechanism of a massive retreat of the coastline over the past thirty years.

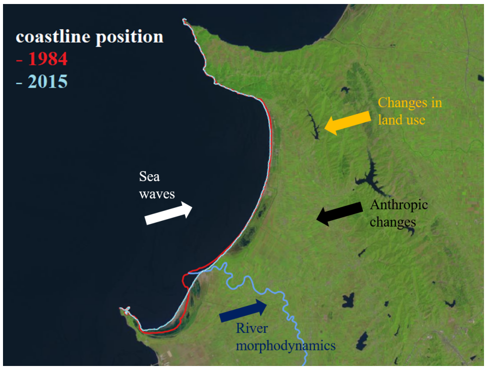

Figure 2. Conceptual diagram of the main geophysical and anthropogenic controls on the coastal dynamics of the Lalzit bay. The red and light blue lines show the temporal variation of the coastline position.

2.2 Field measurements

Field activities were aimed at collecting the minimum required data to investigate the relevant processes affecting coastal dynamics presented in Fig. 2. The geomorphology of the beaches along the bay was characterized through sixteen sections (e.g. Fig. 3) crossing the shoreline, nearly spaced every kilometre along almost twenty km of the bay length (from sec -4, south, to sec 11, north, see Fig. 4A). We recorded the cross-shore section elevation at topographically relevant locations, in correspondence of the main slope changes, with particular attention to the submerged bar system. This allowed to assess the cross-shore sections shape, their berm height and the overall cross-shore profile mean slope (Fig. 3). Moreover, we collected different sand samples along every section to characterize their grain size distribution. Sediment samples were taken at selected locations along each section. Every sand sample was analysed through a multi-filter sieve, to assess the weight percentages of sand in each size class, thus building the grading curve. The obtained data were then post-processed by using the software Gradistat (Blott and Pye, 2001), further evaluating the median grain size (d_{50}) for every sampled location. As the resulting values of d_{50} were not significantly varying along each cross-shore profile, we chose to use those characterizing the water edge foreshore as the representative ones of each section.

Results of the grain size surveys are summarized in Fig. 4. The mean grain size (d_{50}) happens to be quite homogeneous among all the sections (Fig. 4B), and the granulometry of the bay can be considered representative of a “medium sand", according to the classification of Wentworth (1922). The only exception is represented by the section next to the Rodoni cape, which is close to a rocky promontory and is therefore characterized by coarser sediments. On the other hand, cross-shore mean slopes (β_f) and berm heights (B_h) are more variable along the coast, with steeper sections being characterized by lower berms and vice-versa (Fig. 4C, D).

Nat. Hazards Earth Syst. Sci. Discuss., https://doi.org/10.5194/nhess-2018-113
Manuscript under review for journal Nat. Hazards Earth Syst. Sci.
Discussion started: 7 May 2018

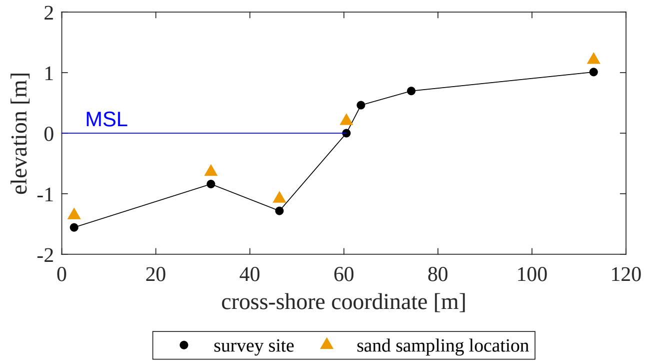

Figure 3. Typical cross-shore profile along the Lazlit Bay (example of section 2, Figure 4A). It is possible to note the presence of the submerged bar some tens of meters away from the coastline

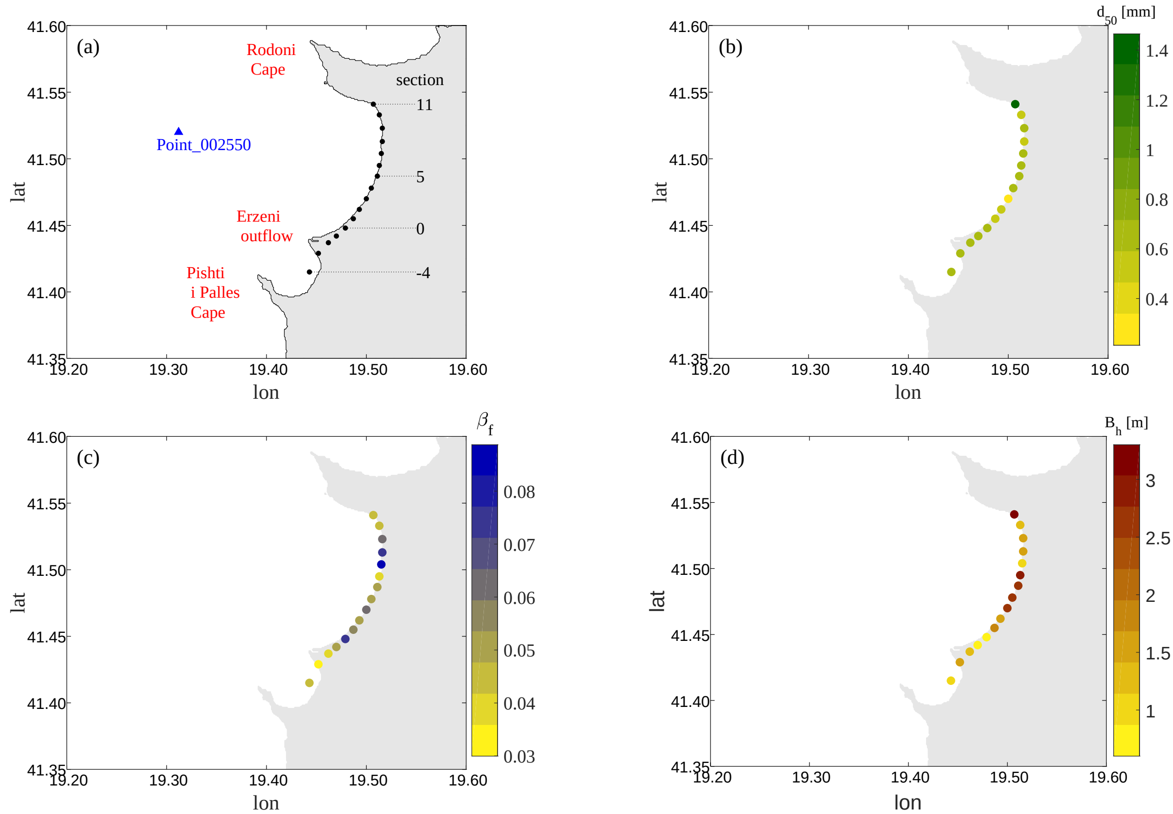

Figure 4. A) Sampling locations for beach sections (from -4 to 11, from south to north), Point_002550 represents DICCA wave hindcast. Spatially distributed values of: B) Median grain size (d_{50}); C) Cross-shore mean slope (β_f); D) Berm height (B_h)

Nat. Hazards Earth Syst. Sci. Discuss., https://doi.org/10.5194/nhess-2018-113
Manuscript under review for journal Nat. Hazards Earth Syst. Sci.
Discussion started: 7 May 2018

2.3 Coastal Vulnerability Indexes (CVI)

CVI are meant to quantify the vulnerability of a coast toward extreme inundation events. For the investigated beach section (or length of shore), a long term statistical computation for the run-up is required, leading to an intermediate dimensionless variable IV (“Inundation Vulnerability"), defined as follows:

$$IV = \frac{Ru_{2\%}}{B_h} \tag{1}$$

where B_h and $Ru_{2\%}$ are the beach berm or dune height and the long term run-up respectively. For each section, the IV value is then evaluated within a given range, obtained by setting two boundary values:

$$\begin{cases} IV_{min} = \dfrac{Ru_{2\%}}{2Ru_{2\%}} \qquad \Rightarrow Ru_{2\%} = 0.5\ B_h \\ \\ IV_{max} = \dfrac{Ru_{2\%}}{Ru_{2\%} - 2} \qquad \Rightarrow Ru_{2\%} = 2 + B_h \end{cases} \tag{2}$$

It can be noticed that the minimum and the maximum vulnerability levels have a clear physical meaning, being explanatory of the cases where the run-up is either half (IV_{min}) of or two meters higher than (IV_{max}) the berm height. This interval is then scaled to a range from 0 to 1, grouped in five classes of equally spaced vulnerability levels (“very low”, ”low”, ”medium”, ”high”, ”very high”) as reported in Table 1.

IV	0 - 0.2	0.2 - 0.4	0.4 - 0.6	0.6 - 0.8	0.8 - 1.0
CVI	very low	low	medium	high	very high

Table 1. Vulnerability levels assessment due to the IV variable

2.4 Wave data and run-up

The assessment of CVI first requires to compute the long term run-up statistics. Regardless the reference model, run-up computation always implies to combine informations about both characteristic wave climate and morphology of a shore (Battjes, 1971; Holman, 1986; Mase, 1989, among others). As regards the wave data, we referred to the hindcast provided by the Department of Civil, Chemical and Environmental Engineering of the University of Genoa (“DICCA", dicca.unige.it/meteocean/hindcast). The hindcast is defined all over the Mediterranean sea from 1979 to 2016 with a 0.1° resolution both in longitude and latitude, one hourly sampled, and it is based on NCEP Climate Forecast System Reanalysis (“CFSR"), for the period from January 1979 to December 2010 and CFSv2 for the period from January 2011 to December 2016 (Mentaschi et al., 2013). The DICCA hindcast was widely validated (Mentaschi et al., 2015), and, being densely defined over a large time period, it helps to perform reliable long-term statistical computations (Coles and Pericchi, 2003). The location we referred to for this study is shown in Fig. 4A (Point_002550), whereas data about the shore geomorphology were collected as explained in Sect. 2.2.

Run-up is therefore computed according to Stockdon et al. (2006) model, as follows:

$$Ru_{2\%} = 1.1 \left\{ 0.35\, \beta_f \sqrt{H_0 L_0} + \frac{\left[H_0 L_0 \left(0.563\, \beta_f^2 + 0.004 \right) \right]^{0.5}}{2} \right\} \tag{3}$$

where β_f stands for the mean slope of the beach, H_0 and L_0 refer to deep water wave height and length respectively.

2.5 Extreme Value Analysis (EVA)

When dealing with run-up estimation, if the data linked to the shore characteristics can be well defined, more uncertainties grow up when trying to empirically parametrize exceptional phenomena (extreme events), of which run-up can be considered as an instance. For this reason we tested two different approaches for the estimation of extreme run-up values.

First, in the frame of a regional analysis, we considered the deep-water data as defined in Point_002550, selecting the annual maxima sea storms from the wave dataset and evaluating the annual maxima run-ups through Eq. (3). This resulted in a 38 extreme run-up dataset for each of the sixteen sections. Every dataset was then modelled through a GEV distribution (Coles et al., 2001), in order to carry out the long term design of run-up values; the validity of the distribution was always proved through the Kolmogorov-Smirnov and the Anderson-Darling parametric tests for every dataset (Massey Jr, 1951; Anderson and Darling, 1954). Given the distributions, we set two target return periods, literally 50 yr and 200 yr, and further computed the resulting run-ups for every section in both cases. This allowed to quantify how CVI estimation could be affected by differently conservative approaches.

Afterwards, we switched from a regional to a locale scale: in this case, EVA were performed directly over the extreme sea storms wave parameters, to assess the 50 yr and the 200 yr waves. We thus propagated the target waves in front of each section, computing afterwards the long term run-up values. Here, as the wave climate shows a clear seasonal dependence with respect to the average incident waves direction, we splitted the initial wave dataset according to two meaningful directional fetches; this choice involved two important consequences.

First, when performing directional analysis, referring return periods for each of the identified sectors have to be carefully assigned, as demonstrated by Forristall (2004):

$$\begin{cases} F_o = \prod_1^N F_i \\ 1 - \dfrac{1}{\lambda_o T_{R_o}} = \prod_1^N \left(1 - \dfrac{1}{\lambda_i T_{R_i}} \right) \end{cases} \tag{4}$$

being F the probability of non exceedance, λ the yearly number of extreme events, T_R the significant return period; subscripts o and i stand for omnidirectional and the i^{-th} directional pattern, respectively. The F_i probabilities are fixed in order to obtain N equal values whose product gives F_o. This precaution is due to the fact that, when referring to an omnidirectional analysis, a higher number of events is expected compared to the case of a directional analysis, thus a higher probability of non exceedance (see Eq. (4)). Multiplying the probabilities related to the identified sectors ensures a coherent computational procedure; we therefore previously fixed the referring non-exceedance probability for each sector, in order to get an overall value equal to that of the omnidirectional analysis (given the referring T_{R_o}).

Moreover, referring to a subset of the whole dataset implies a lower amount of data to deal with. In order to overcome this drawback, we used the Peaks Over Threshold (POT) approach to come up with long term wave height estimates, imposing a threshold value of 3 m and a minimum inter-event duration of $24\mathrm{hr}$; threshold values were set to get datasets characterized by events being independents and identically distributed, as specified by Lang et al. (1999). Probabilities obtained with Eq. (4) lead to the long term significant wave heights; in this case we adopted a Weibull distribution applied to the exceedances of the given threshold, as specified in DNV (2010), testing as well the suitability of the distribution as performed for the regional analysis. To completely characterize the target waves (to be downscaled at a later time in the near-shore zone), we linked the peak periods to the computed significant wave heights according to the empirical formula of Callaghan et al. (2008); the mean directions were assessed instead due to the particular waves climate of the area. Resulting values were set as inputs to the SWAN model (Booij et al., 2003), allowing to get the parameters at a depth of ten meters in front of each of the investigated sections. The obtained wave parameters were then used to compute the 10 m depth run-up for both the considered return periods. As regards the bathymetry of the bay, we referred both to the ETOPO1 dataset (www.ngdc.noaa.gov) and a nautical chart of the Italian Hydrographic Institute (www.marina.difesa.it).

It is worth mentioning that the return period of a forcing variate is not necessarily equal to the return period of the outcomes (Hawkes et al., 2002); as an instance, a given return period wave may not lead to the corresponding return period run-up. Anyway, Garrity et al. (2007) demonstrated that this approach can still leads to satisfactory results, and it has already been adopted within previous studies (Vitousek et al., 2008).

3 Results

Once we computed the long term run-ups, we evaluated the resulting CVI according to the morphology of the testing locations. Since results are punctual (e.g. one index for each of the sixteen sampling locations). We linearly interpolated the IV values within hypothetical intermediate sections, in order to get a more meaningful overview about the whole bay.

We initially referred to the regional scale; in this case, an omnidirectional analysis was performed, leading to two sets of results linked to the tested return periods. Secondly, we detailed our study to the local scale: in this case, we got two sets of results for every directional sector taken into account. We first present the CVI obtained from the regional study.

3.1 Regional scale (offshore wave conditions)

At the regional scale the environmental inputs were the same for each section, being the wave characteristics defined in deep water (Point_002550, Fig. 4A); the differences in the run-up significant values were just due to different morphological characteristics of each cross-shore section (literally, the mean slope of the different beach profiles). This can be clearly noticed in Fig. 5: the empirical run-ups show the same distribution for every section, as their values are just rigidly translated of a quantity that depends on the value of the section slope β_f (see Eq. 3). From the curves in Fig. 5, the run-ups linked to 50 and 200 yr return period were extrapolated, and the inundation vulnerability indexes were accordingly computed, as explained in section

2.3. Results are shown in Fig. 6.

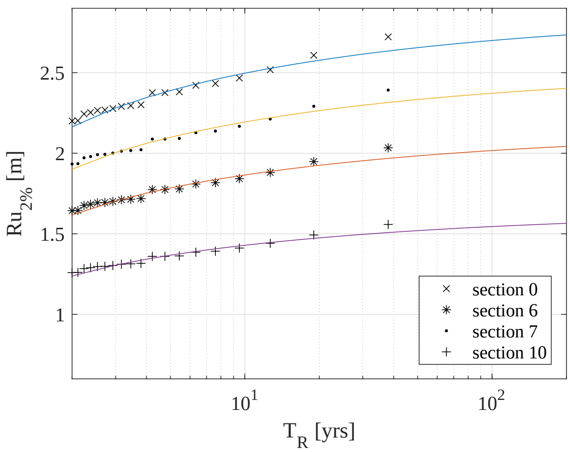

Figure 5. Return period curves for the run-up parameter; results are presented for just some of the cross-sections for the sake of clarity

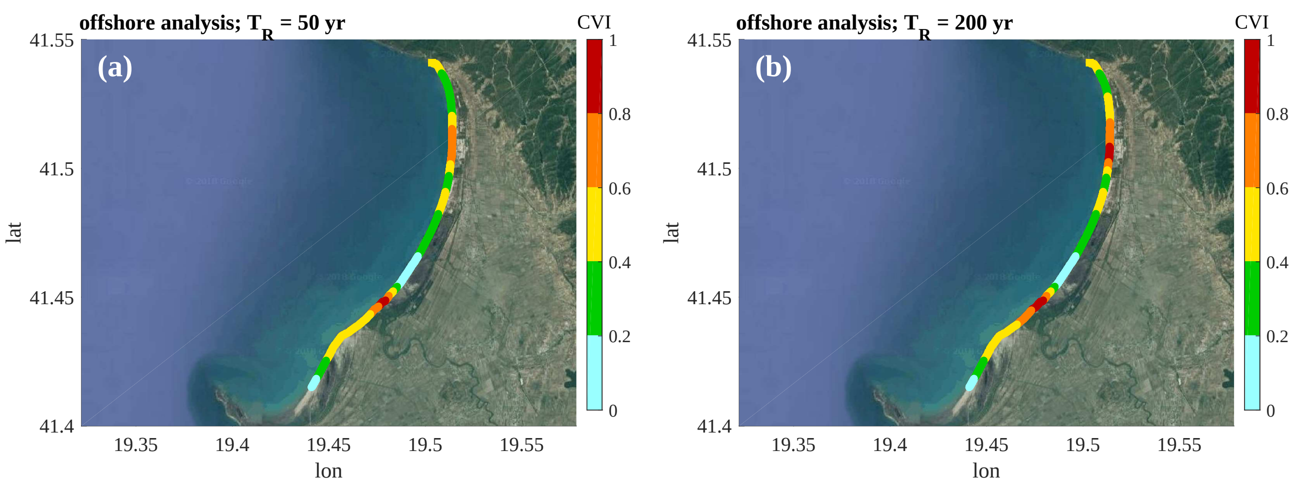

Figure 6. Run-up vulnerability indexes for the Lalzit Bay from the regional analysis, using deep water data: A) 50 yr return period; B) 200 yr return period

Nat. Hazards Earth Syst. Sci. Discuss., https://doi.org/10.5194/nhess-2018-113
Manuscript under review for journal Nat. Hazards Earth Syst. Sci.
Discussion started: 7 May 2018

3.2 Local scale (nearshore wave conditions)

Evaluation of coastal vulnerability indexes has been carried out also by employing the propagated values of the wave climate at the local scale. It has to be remarked that, in this case, the mean cross-shore slope is not the only changing parameter between one section and another: as waves are propagated toward the shore in front of each of the investigated locations, they are modified due to the occurring transformation processes, resulting in different wave characteristics (heights, lengths and incident directions) depending on the position of a section along the bay.

The first step to compute the indexes at a local scale is to characterize the wave climate. We mainly referred to the significant wave height, looking at the distribution of the waves incoming direction over different seasons. As shown in Fig. 7, the wave climate of the Lalzit bay is characterized by a strong seasonal behaviour: during the summer months, the prevalent incoming direction happens to be W-NW, whereas for the other seasons waves mainly come from the S-SW direction. We therefore considered two directional sectors, 250-350° N and 190-250° N, being representative of summer and of the rest of the year, respectively.

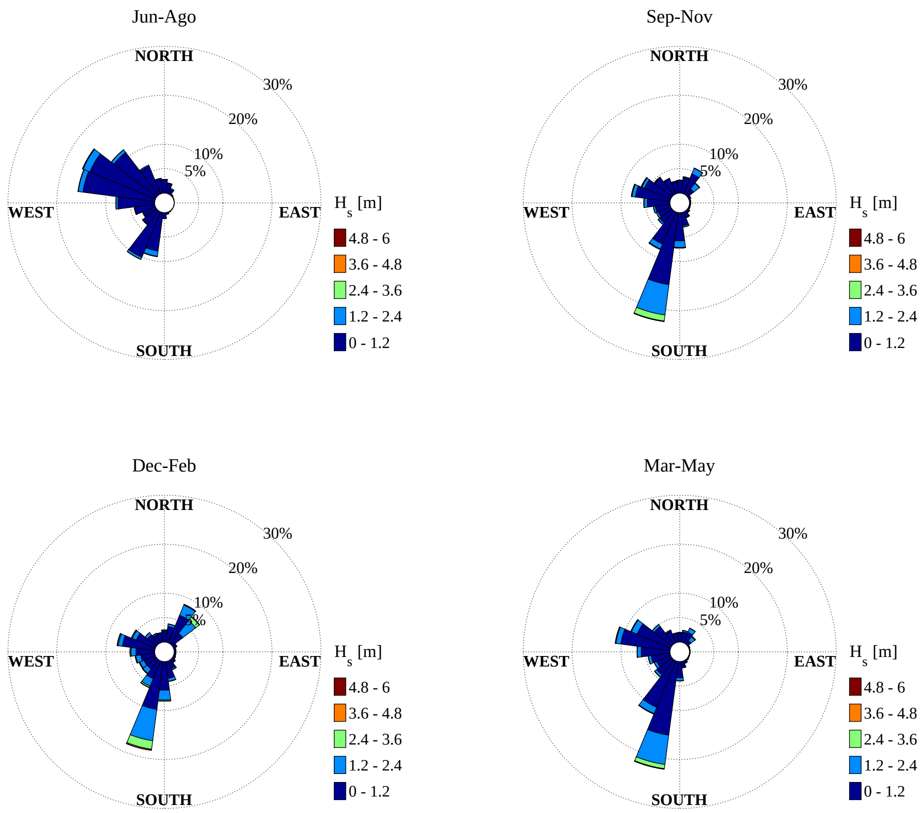

Figure 7. Seasonal roses of significant wave height for hindcast Point_002550.

Nat. Hazards Earth Syst. Sci. Discuss., https://doi.org/10.5194/nhess-2018-113
Manuscript under review for journal Nat. Hazards Earth Syst. Sci.
Discussion started: 7 May 2018

Extreme events have been defined for each of the identified sectors, computing the resulting 50 yr and 200 yr return period wave heights. The target wave incoming direction for each sector was defined through a linear interpolation, in order to minimize the root mean square error with respect to the directions of the sea storms identified with the POT approach (see Fig. 8). Finally, for the wave periods, we referred to the empirical equation of Callaghan et al. (2008):

$$\begin{cases} E(T_p) = aH_s^b + cfH_s^{d+g} \\ a = 3.005; b = 0.543; c = 4.82; d = -0.332; f = 1.122; g = -0.039 \end{cases} \tag{5}$$

where H is the target wave height computed through the POT approach, as previously explained; a, b, c, f, d and g are given parameters.

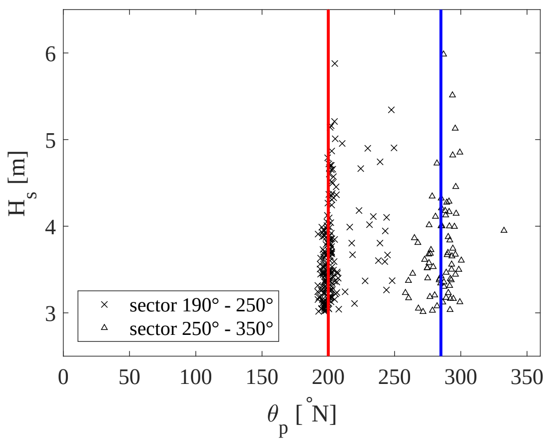

Figure 8. Directions of the extremes waves extracted through the Peaks Over Threshold procedure.

We therefore characterized the design wave for each of the identified directional sectors (W-NW and S-SW), defining its significant height, peak period and angle of attack. These parameters were set at a time as inputs of the wave propagation model, in order to get the shallow water wave parameters. The starting values are shown in Table 2. The inundation vulnerability indexes following the downscaled wave features are shown in Fig. 9 and 10.

sector [°N]	T_R [yrs]	H_s [m]	T_p [s]	θ_p [°N]
190-250	50	6.49	11.0	200
	200	7.01	11.3	200
250-350	50	6.64	11.1	285
	200	7.17	11.4	285

Table 2. Design wave parameters for the seasonal directional sectors. Notations T_R is the return period, H_S, T_P, and θ_P stand for wave height, period and incoming direction, respectively.

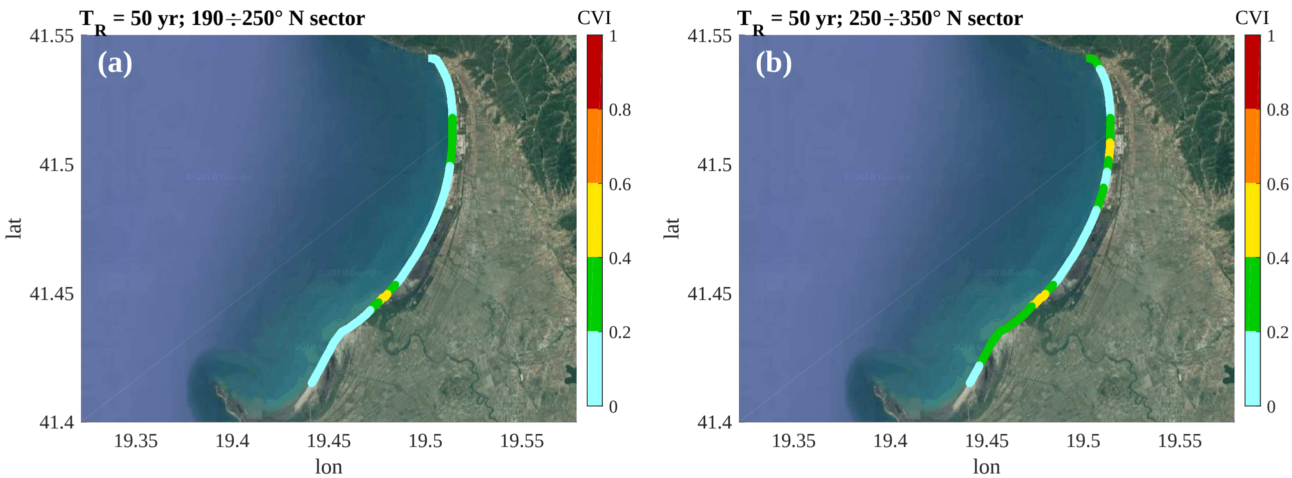

Figure 9. Run-up vulnerability indexes for the Lalzit Bay, using near-shore data for the 50 yr return period for different directional patterns: A) 190-250°N sector; B) 250-350°N sector.

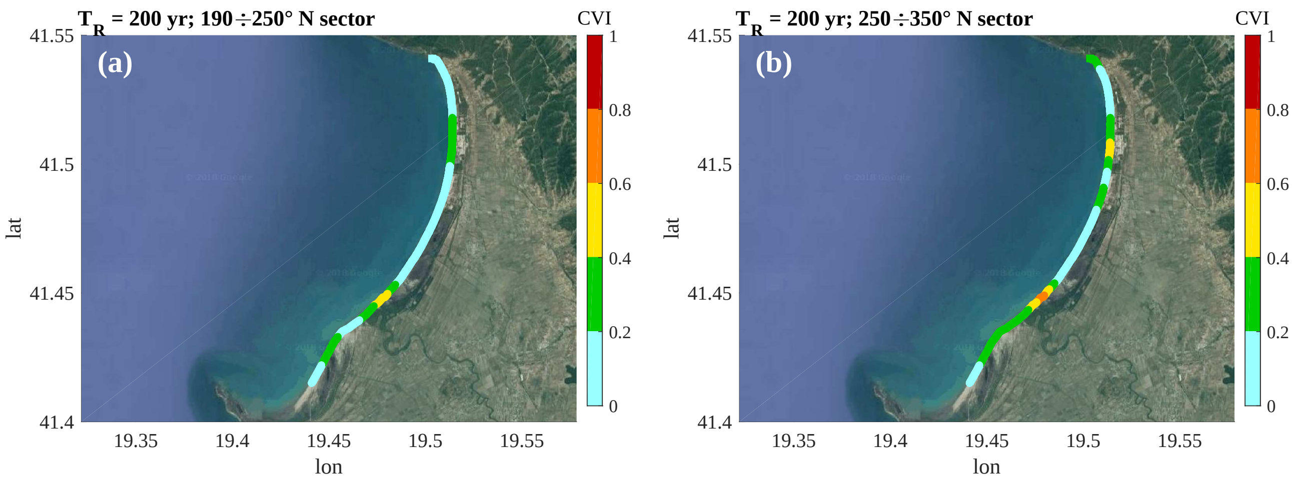

Figure 10. Run-up vulnerability indexes for the Lalzit Bay, using near-shore data for the 200 yr return period for different directional patterns: A) 190-250°N sector; B) 250-350°N sector.

For the sake of clarity, in order to compare the results obtained with the two different approaches mentioned before, we discuss just the results linked to the punctual investigated sections; analogous considerations can be therefore extended to the intermediate sections, whose vulnerability levels were assessed through a linear interpolation as previously explained.

Looking at the punctual results (Fig. 11 and 12), it can be noticed that in all considered cases even sections lying next to each other can show very different vulnerability levels: as the sampling locations are 1 km distant one from another, their morphological characteristics can significantly vary, and this is consequently reflected in the results.

Nat. Hazards Earth Syst. Sci. Discuss., https://doi.org/10.5194/nhess-2018-113
Manuscript under review for journal Nat. Hazards Earth Syst. Sci.
Discussion started: 7 May 2018

Referring to the regional scale-offshore analysis and 50 yr return period, the vulnerability towards inundation happens to be “very high" in section 0, and still “high" in sections 7, 8; sections -4, 1, 2 are characterized by a “very low" vulnerability, whereas sections 3, 4, 6, 9 and 10 show “low" vulnerability; the other ones are characterized by a “medium" vulnerability. As we could expect, vulnerability levels increase when referring to 200 yr return period: in this case, a “very high" vulnerability characterizes section 7 as well, whereas the level increase from “medium" to “high" in section -1, and from “low" to “medium" in section 9; vulnerability class does not change for sections -4, -3, -2, and for sections between 0 and 6.

The directional analysis indicates that results are less varying with respect to the return period: if we refer to the 190-250° N sector, 50 yr return period, vulnerability levels are “very low" for all sections but 7 and 8, which show “low" vulnerability, and 0 (“medium vulnerability"). Switching to the 200 yr return period, vulnerability rises from “very low" to “low" in sections -3, -1, being unvaried in all the other ones. Results are slightly different for the 250-350° N sector: in this case, 50 yr vulnerability is “low" (instead of “very low") for sections -3, -2, -1, 5, 11; section 7 shows a “medium" instead of a “low" vulnerability. Again, results proportionally increase due to the considered return period: differences between the previous directional sector can be noted in section -2, 5, 11, being characterized by a “low" vulnerability rather than by a “very low" one; sections 0 and 7 are respectively “high" and “medium" vulnerable, whereas they are characterized by a one step lower vulnerability levels compared to S-SW fetch.

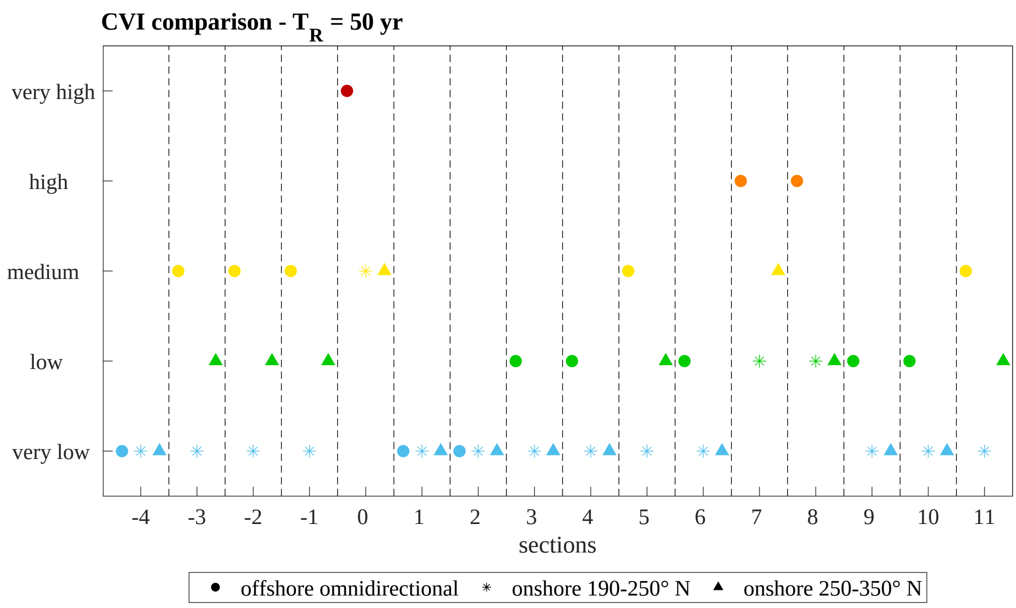

Figure 11. Comparison between the run-up vulnerability indexes for each sampling location; return period equal to 50 yr.

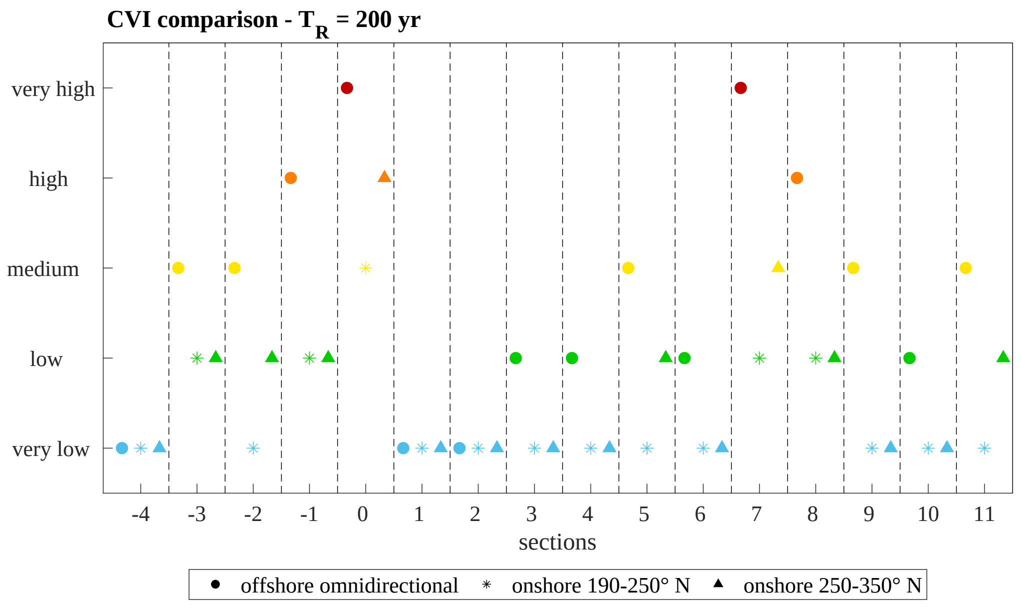

Figure 12. Comparison between the run-up vulnerability indexes for each sampling location; return period equal to 200 yr.

It is interesting to evaluate how CVI can change due to the starting wave features: the extreme value analysis performed using deep-water data yields higher vulnerability levels than those obtained after propagating waves toward the shore. Referring to 50 yr return period, the most exposed sections are yet characterized by “very high" (0) and “high" (7, 8) levels of vulnerability, whereas is just considering the 200 yr return period that the directional analysis lead to a “high" level (section 0, 250-350° N sector); in this case, through omnidirectional analysis sections 7 and -1 become “very high" and “high" vulnerable respectively, whereas the directional analysis carries vulnerability levels never higher than “medium" but that of section 0, precisely.

Actually, results divergence decreases for sections characterized by “low" and “very low" vulnerability levels: in this case, the morphology of the surrounding beach seems to guarantee safe conditions, regardless to the magnitude of the forcing wave.

4 Discussion

As a general trend, assessing coastal vulnerability to inundation using the wave climate computed at the local scale leads to lower vulnerability levels compared to those obtained through the regional analysis. If the vulnerability levels are similarly distributed along the bay (depending on the single section profiles), the long term run-up estimates are clearly dependent to the referring spatial scale: the geometry of the bay indeed strongly affects the waves’ propagation toward the coast. Moving onshore, in the Lalzit bay wave heights likely decrease due to refraction and diffraction, which can be expected to be the dominant processes as suggested by the concave enclosed shape of the coast. Consequently, run-up estimates come to be lower when dealing with the local-scale analysis, and resulting CVI behave accordingly. Results reported in Fig. 11 and 12 highlight

Nat. Hazards Earth Syst. Sci. Discuss., https://doi.org/10.5194/nhess-2018-113
Manuscript under review for journal Nat. Hazards Earth Syst. Sci.
Discussion started: 7 May 2018

another important aspect: if we refer to the local scale, the vulnerability of the bay as a whole is higher when looking at the summer months (250-350°N). This outcome is justified as well by the geometry of the bay, in fact, even if the starting wave features for the different directional frames are similar (Table 2), waves coming from W-NW are not diffracted by the southern cape as it happens instead for those coming from S-SW. The absence of obstacles along the waves path implies a lower reduction of the wave heights, involving in turn higher values of the following run-ups, thus higher values for the IV variables (see Fig. 13A, B).

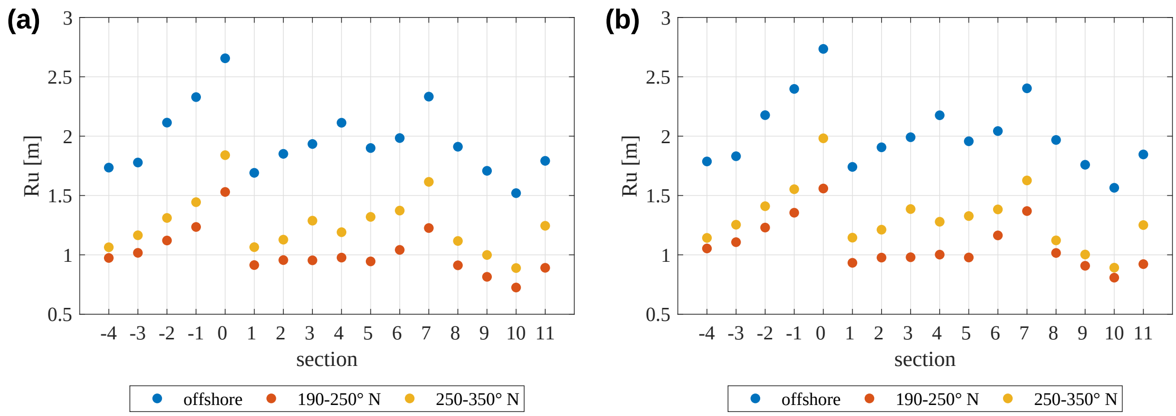

Figure 13. Comparison between run-up values for each section obtained through offshore (regional scale) and near-shore (local scale) conditions: A) $50yr$ return period; B) $200yr$ return period

Higher run-up estimates due to offshore analysis suggest another consideration about the different variability of the results between regional (offshore) and local (onshore) analysis: as previously demonstrated, the directional data result in a more homogeneous vulnerability level along the coastline. This can be simply justified looking at the vulnerability level computation: the same IV index may belong to different vulnerability classes, depending on the value that the IV_{max} variable gets; in fact, while IV_{min} is constant for any of the investigation approaches, the maximum IV depends on the run-up values (see Eq. (2)). High run-up imply lower IV_{max} values, thus a lower total range, which, being spaced in five classes anyway, leads to narrower intervals. Resulting vulnerability levels are therefore more sensitive to smaller variations of the IV values (as Fig. 11 and 12 show).

Finally, if we enlarge our analysis to the coastline as a whole, we can better appreciate how vulnerability is distributed. Despite the differences due to the referring wave data, the most vulnerable areas happen to be those nearby the Erzeni outflow and, in the north, toward the Rodoni cape (see Fig. 4A for references), even if for different causes. If we look at the berm height component, it is evident how the aforementioned areas are characterized by lower berms (Fig. 4D): the Erzeni outflow area has shown in the last years a significant ongoing coastal erosion, as it is estimated that the coastline is retreating at a speed of 0.3÷0.5 $\mathrm{m/y}$ (Boçi, 1994), resulting in the berms levelling; actually, the concurring reduction of the river sediment transport has also implied steeper profiles (Fig. 4C), that lead to higher run-up estimates. Moving to the north, the lower berms are due instead to the anthropic activities recently developed, which required the levelling of the beach as well; concerning the cross-shore slope, there is actually no evidence of steeper profiles but that of section 7.

5 Conclusions

The vulnerability assessment of a coastline can be a helpful device to plan its land use, as an instance not considering to place high value activities when there's a high risk for the beaches of being submerged or eroded. In this framework, CVI provide an easy and reliable tool, in order to get an overall overview about a shore vulnerability distribution toward either inundation and/or erosion events.

In this paper, we evaluated the coastal inundation vulnerability for the bay of Lalzit (Durrës, Albania), following the model proposed by Bosom García and Jiménez Quintana (2011). We first performed a regional analysis, referring to the original formula of Stockdon et al. (2006) in order to compute the extreme values for the run-ups at sixteen sections along the bay; then, we detailed the study downscaling the wave features in the shallow waters thanks to a wave propagation model.

We showed that, even if the vulnerability distribution do not change along the shore (e.g. the most exposed sections are placed in the same areas), the results linked to the local scale yield considerably lower vulnerability levels. This is mainly due to the run-up estimates, which are very sensitive to the input wave characteristics, which may be defined in shallow or deep waters. In the case of Lalzit, when waves propagation processes (such as refraction and breaking) become influential, run-up estimates can considerably change depending on the level of detail of wave characterization, as vulnerability levels accordingly do.

Since the model of Stockdon et al. (2006) quantifies extreme values for the run-up variable, it appears more plausible to refer to the modified model as proposed by Sancho-García et al. (2012), to link it with high return period, without computing extreme analysis twice at a time. This precaution may allow to get more reliable CVI assessment, properly scaling their related values due to the chosen return period. A critical analysis of the coastline vulnerability could prevent to adopt too much conservative approaches, that could lead to unnecessary countermeasures, translating to loss of money and invasive non required interventions.

The feasibility of CVI assessment can represent a crucial ingredient for rapidly developing and transforming coastal regions such as the Lalzit bay in Albania, which present more options to drive virtuous future coastal development compared to industrialized countries, where CVI assessment may mostly represent a tool for ICZM applied to manage conflicts among relevant stakeholders.

Acknowledgements. This study is part of a project shared between the University of Trento and the University of Genoa (Italy), along with the Polytechnic of Tirana (Albania). The authors would like to thank everyone who joined the field data collection: Alessandro Chesini, Alessandro Dotto, Alessio Maier, Daniele Spada, Dario Guirreri, Erasmo Vella, Federica Pedon, Giorgio Gallerani, Laura Dalla Valle, Martina Costi, Navarro Ferronato, Stefano Gobbi, Tommaso Tosi (University of Trento), Ardit Omeri, Arsela Caka, Bardhe Gjini, Bestar Cekrezi, Erida Beqiri, Ferdinand Fufaj, Idlir Lami, Marie Shyti, Mikel Zhidro, Nelisa Haxhi, Xhon Kraja, Tania Floqi (Tirana Polytechnic). The collected data were then analysed by the Italian partners, in the framework of the UNESCO Chair in Engineering for Human and Sustainable Development (DICAM-Unesco Chair). G. Besio has been funded by University of Genoa through “Fondi per l’Internazionalizzazione" grant.

References

Anderson, T. W. and Darling, D. A.: A test of goodness of fit, Journal of the American statistical association, 49, 765–769, 1954.

Armaroli, C. and Duo, E.: Validation of the coastal storm risk assessment framework along the Emilia-Romagna coast, Coastal Engineering, 2017.

Battjes, J. A.: Run-up distributions of waves breaking on slopes, Journal of Waterways and Harbors Division, 97, 1971.

Blott, S. J. and Pye, K.: GRADISTAT: a grain size distribution and statistics package for the analysis of unconsolidated sediments, Earth surface processes and Landforms, 26, 1237–1248, 2001.

Boçi, S.: Evoluzione e problematiche ambientali del litorale albanese, Bollettino della Societa Geologica Italiana, 113, 7–14, 1994.

Booij, N., Ris, R., and Holthuijsen, L.: A third-generation wave model for coastal regions, J. Geophys. Res., 104, C4, 2003.

Bosom García, E. and Jiménez Quintana, J. A.: Probabilistic coastal vulnerability assessment to storms at regional scale: application to Catalan beaches (NW Mediterranean), Natural hazards and Earth system sciences, 11, 475–484, 2011.

Callaghan, D., Nielsen, P., Short, A., and Ranasinghe, R.: Statistical simulation of wave climate and extreme beach erosion, Coastal Engineering, 55, 375–390, 2008.

Ciccarelli, D., Pinna, M., Alquini, F., Cogoni, D., Ruocco, M., Bacchetta, G., Sarti, G., and Fenu, G.: Development of a coastal dune vulnerability index for Mediterranean ecosystems: A useful tool for coastal managers?, Estuarine, Coastal and Shelf Science, 187, 84 – 95, 2017.

Coles, S. and Pericchi, L.: Anticipating catastrophes through extreme value modelling, Journal of the Royal Statistical Society: Series C (Applied Statistics), 52, 405–416, 2003.

Coles, S., Bawa, J., Trenner, L., and Dorazio, P.: An introduction to statistical modeling of extreme values, vol. 208, Springer, 2001.

De Leo, F., Besio, G., Zolezzi, G., Bezzi, M., Floqi, T., and Lami, I.: Coastal erosion triggered by political and socio-economical abrupt changes: the cse of Lalzit Bay, Albania, Coastal Engineering Proceedings, 1, 13, 2017.

Di Paola, G., Aucelli, P. P. C., Benassai, G., and Rodríguez, G.: Coastal vulnerability to wave storms of Sele littoral plain (southern Italy), Natural hazards, 71, 1795–1819, 2014.

Di Risio, M., Bruschi, A., Lisi, I., Pesarino, V., and Pasquali, D.: Comparative Analysis of Coastal Flooding Vulnerability and Hazard Assessment at National Scale, Journal of Marine Science and Engineering, 5, 2017.

DNV, D.: C205 Environmental conditions and environmental loads, Recommended Practice, 2010.

Ferreira Silva, S., Martinho, M., Capitão, R., Reis, T., Fortes, C., and Ferreira, J.: An index-based method for coastal-flood risk assessment in low-lying areas (Costa de Caparica, Portugal), 114, 90–104, 2017.

Fitton, J. M., Hansom, J. D., and Rennie, A. F.: A national coastal erosion susceptibility model for Scotland, Ocean and Coastal Management, 132, 80 – 89, 2016.

Forristall, G. Z.: On the use of directional wave criteria, Journal of waterway, port, coastal, and ocean engineering, 130, 272–275, 2004.

Garrity, N. J., Battalio, R., Hawkes, P. J., and Roupe, D.: Evaluation of event and response approaches to estimate the 100-year coastal flood for Pacific coast sheltered waters, in: 30th International Conference on Coastal Engineering, ICCE 2006, 3 September 2006 through 8 September 2006, San Diego, CA, United States, pp. 1651–1663, 2007.

Hawkes, P. J., Gouldby, B. P., Tawn, J. A., and Owen, M. W.: The joint probability of waves and water levels in coastal engineering design, Journal of hydraulic research, 40, 241–251, 2002.

Holman, R.: Extreme value statistics for wave run-up on a natural beach, Coastal Engineering, 9, 527–544, 1986.

Kamphuis, J. W.: Introduction to coastal engineering and management, vol. 30, World Scientific Publishing Co Inc, 2010.

Lang, M., Ouarda, T., and Bobée, B.: Towards operational guidelines for over-threshold modeling, Journal of hydrology, 225, 103–117, 1999.

Mase, H.: Random Wave Runup Height on Gentle Slope, Journal of Waterway, Port, Coastal, and Ocean Engineering, 115, 649–661, 1989.

Massey Jr, F. J.: The Kolmogorov-Smirnov test for goodness of fit, Journal of the American statistical Association, 46, 68–78, 1951.

Mavromatidi, A., Briche, E., and Claeys, C.: Mapping and analyzing socio-environmental vulnerability to coastal hazards induced by climate change: An application to coastal Mediterranean cities in France, Cities, 72, 189 – 200, 2018.

Mentaschi, L., Besio, G., Cassola, F., and Mazzino, A.: Developing and validating a forecast/hindcast system for the Mediterranean Sea, Journal of Coastal Research, SI 65, 1551–1556, 2013.

Mentaschi, L., Besio, G., Cassola, F., and Mazzino, A.: Performance evaluation of WavewatchIII in the Mediterranean Sea, Ocean Modelling, 90, 82–94, 2015.

Montreuil, A.-L., Chen, M., and Elyahyioui, J.: Assessment of the impacts of storm events for developing an erosion index, Regional Studies in Marine Science, 16, 124 – 130, 2017.

Narra, P., Coelho, C., Sancho, F., and Palalane, J.: CERA: An open-source tool for coastal erosion risk assessment, Ocean and Coastal Management, 142, 1 – 14, 2017.

Neumann, B., Vafeidis, A. T., Zimmermann, J., and Nicholls, R. J.: Future coastal population growth and exposure to sea-level rise and coastal flooding-a global assessment, PloS one, 10, e0118 571, 2015.

Sancho-García, A., Guillén, J., Simarro, G., Medina, R., and Cánovas, V.: Beach inundation prediction during storms using direferents wave heights as inputs, International Conference on Coastal Engineering, 2012.

Satta, A., Snoussi, M., Puddu, M., Flayou, L., and Hout, R.: An index-based method to assess risks of climate-related hazards in coastal zones: The case of Tetouan, Estuarine, Coastal and Shelf Science, 175, 93–105, 2016.

Óscar Ferreira, Plomaritis, T. A., and Costas, S.: Process-based indicators to assess storm induced coastal hazards, Earth-Science Reviews, 173, 159 – 167, 2017.

Soukissian, T. H., Ntoumas, M. C., Anagnostou, C., Kiriakidou, C., et al.: Coastal Vulnerability of Eastern Saronikos Gulf to intense natural events, in: The Twentieth International Offshore and Polar Engineering Conference, International Society of Offshore and Polar Engineers, 2010.

Stockdon, H., Holman, R., Howd, P., and Sallenger Jr., A.: Empirical parameterization of setup, swash, and runup, Coastal Engineering, 53, 573–588, 2006.

UNEP, M.: ICZM Protocol in the Mediterranean, available at: www. pap-thecoastcentre. org, 2008.

Vitousek, S., Fletcher, C. H., and Barbee, M. M.: A practical approach to mapping extreme wave inundation: Consequences of sea-level rise and coastal erosion, in: Solutions to Coastal Disasters 2008, pp. 85–96, 2008.

Wentworth, C. K.: A scale of grade and class terms for clastic sediments, The Journal of Geology, 30, 377–392, 1922.

Dear Editor,

we would like to thank the reviewers for their effort in reading and commenting the paper. We went through all the comments and we tried to answer in detail to all of them. An item-by-item reply follows for the Reviewer 1 revision. For those comments on which we could not agree, a detailed rebuttal is presented in the reply which follows.

REVIEWER 1

We thank the Reviewer for his interest in our paper and for his criticism. We have considered all the review comments and undertaken a major revision, incorporating nearly all the requested changes into the manuscript.

---

[1] *The first comment is purely formal. Although the index used by authors can formally be denoted as a coastal vulnerability index, I recommend authors to do not use CVI to refer to the index to avoid misunderstandings with readers since CVI is usually employed to name the Coastal Vulnerability Index developed by Gornitz et al. (1994) and all variations used by USGS and others. Take this in consideration and apply throughout the manuscript.*

We recognize that the notation "CVI" was originally defined for the index of Gornitz et al. (1994) and its variations; actually, we were keeping this notation as there are other studies presenting the development of Coastal Vulnerability Indexes literally named as CVI, even though the proposed methodology does not precisely follow that of Gornitz et al. (1994) (see, as an instance, Kumar et al., 2010; McLaughlin et al., 2002, among others)

Anyway, in order to avoid any possible misunderstanding, we decided not to longer use the notation "CVI", speaking instead of "vulnerability level" (or "VL") of the coast. We therefore changed it throughout the whole paper.

---

[2] *Lines 14-18 (pag 2). The interpretation of the runup model of Stockdon et al. (2006) does not seem to be formally correct. The 2% factor is common to many of runup models (and, probably, the most used statistical value in flood-hazard assessments), and it refers the value exceeded by 2% of the runup values induced during a given wave-state (which is characterized by the use of Hs). In essence, the idea is to select a statistical description of the runup distribution (induced by the random wave state) and its selection will depend on the objective of the analysis. This 2% does not refer to probability of exceedance or return period as the text seems to suggest.*

We acknowledge that the explanation is a little bit confusing; clearly the return period of an event is linked to its probability of non-exceedance among the distribution it may belong to, but this applies in the frame of EVA. In this case, the 2% refers instead to the distribution of a single sea state, so it cannot be linked to any return period, as the referee correctly pointed out. However, this percentage is actually tied to a probability of exceedance, as "it refers to the value exceeded by 2% of the runup values induced during a given wave-state" (according to the referee's comment); thus, it represents a high quantile among a hypothetical series of observed runup values during a sea state. Through the propagation of the waves at a 10m depth, we are referring instead to an *expected value* of a sea state induced run-up (as proved by Sancho-García et al., 2012), to see how a different approach may affect the computation of the resultant vulnerability levels.

The discussion has been changed in lines 13-20 of pag.2, in order to better clarify the differences between the two approaches.

---

[3] *Lines 18-24 (pag 2). This type of observation has also been previously done for other runup models. It is due to the fact that if the model is going to be fed with deepwater input data (as it is the case of most of runup models), if wave conditions significantly modify during propagation (diffraction, irregular bathymetry), used data will not properly represent real nearshore conditions. In any case and, just regarding the use of the Stockdon runup model, I include here two references that can be helpful.*
Plant & Stockdon. (2015). How well can wave runup be predicted? Comment on Laudier et al. (2011) and Stockdon et al.(2006). Coastal Engineering, 102, 44-48.
Stockdon et al (2014). Evaluation of wave runup predictions from numerical and parametric models. Coastal Engineering, 92, 1-11.

We appreciate the suggestions.

As regard the paper of Plant and Stockdon (2015), we precise that we used the full parametrization of Stockdon et al. (2006) as the authors suggest; moreover, the beach of the Lalzit bay is barred, so no hypothetical additional sources of uncertainty may exist (as Laudier et al., 2011, suggested comparing the Stockdon et al. (2006) model performances on non-barred beaches).

Looking instead at Stockdon et al. (2014), a comparisons for swash and setup values between Stockdon et al. (2006) and the XBeach simulations for "extreme conditions" was carried out, in order to evalute the applicability of Stockdon et al. (2006) for very intense sea states: results were consistent for infragravity swash, while for the setup they agree just for the category I storm (defined according to the Saffir-Simpson scale). Nevertheless, in the Adriatic Sea, climate is never characterized by winds belonging to the higher categories, so that we can use this reference to justify the use of Stockdon et al. (2006) for the local extreme sea states of the bay of Lalzit.

Finally, according to the references proposed by the reviewer, we are referring to the Stockdon et al. (2006) parametrization as "S2006".

---

[4] *Line1 (pag 3). The right cite of Bosom García and Jiménez Quintana (2011) is Bosom and Jiménez 2011). Please change through the manuscript.*

Thank for pointing it out (we used the pre-defined settings of the Copernicus package as suggested by the Journal). The typo has been fixed throughout the paper.

---

[5] *Section 2.3 (pag 6). Please mention that this is (or it is based on) the index/method proposed by Bosom and Jiménez (2011).*

Amended as suggested.

---

[6] *Lines 9-10 (pag 6). Please be explicit with the "physical meaning" of used intervals. (e.g something like this... The minimum value corresponds to a configuration in which the beach is not overtopped and, in consequence, the hinterland is well protected from inundation for the tested conditions. On the other hand, the maximum value...).*

Amended as suggested: the meaning of the term is explained at line 10, pag. 6.

---

[7] *Lines 8-9 (pag 7). With this approach you are assuming that the probability of the hazard (runup) is the same that the probability of the wave height. However, this is not exactly true since Ru depends on Hs and Tp. The strict way to obtain the 38-year time-series of annual maxima Ru, will be to compute Ru of all conditions during each year and to retain the maximum value every year.*

We agree on that; we used this analysis to ensure a coherent comparison with the results due to the propagation of waves towards the coast. In this last case, according to the referee comment, we would have had to compute the long term run-up starting from the whole series of propagated waves parameters; nevertheless, to downscale 38 years of hourly defined wave data may be computationally too expensive. Therefore, when dealing with the off-shore analysis, we first evaluated the 38 maxima runup due to the "strict way" as explained in the referee's comment; then, we compared these values with those computed according to the procedure explained in the paper (lines 8-9, pag.7). This analysis was performed for each of the sixteen locations, the results for the less steep and the steepest sections are shown in Figure 1 of the present reply.

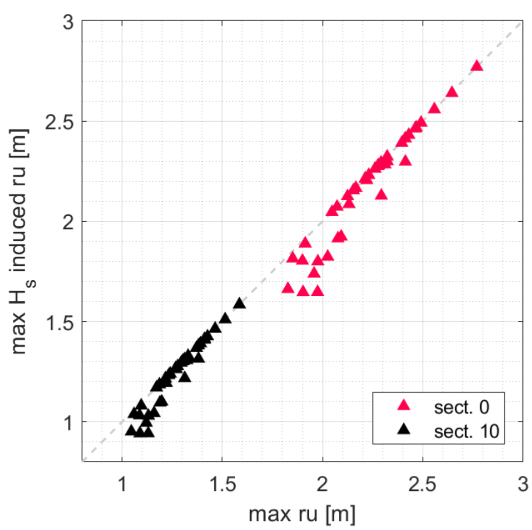

Figure 1: Yearly maxima run-up comparison for the sections characterized by the minimum and the maximum slope (10 and 0, respectively).

Actually, the two approaches for run-up computation lead to similar results, and this is reflecting on the long-term curves which happen to lie very close to each other; therefore, resultant vulnerability levels are not sensitive to the selected approach for our case study. Then, even though there is no evidence that the same would occur with the directional onshore analysis, there is no reason for us to expect huge divergences. Moreover, the same kind of analysis has been previously performed in other papers, as reported in the manuscript (lines 14-17, pag.8). We decided not to put these results for the sake of breavity, nonetheless we are commenting them at the end of line 9, pag.7.

---

[8] *Line 14-15 (pag 7). The use of a given Tr is not conservative by itself. The appropriateness of the used value will depend on the safety level of the analysis (which should be related to the value of the hinterland potentially exposed to inundation).*

We agree with the reviewer that a referring return period has to be defined according to a required safety level. Here, beside the characterization of the vulnerability levels for the bay of Lalzit, we want to show how to rely on a regional or a local scale may affect these levels themselves. For a more meaningful overview, we referred to two different return periods, explanative of two different hypothetical safety levels: that's the reason for that we talk about "differently conservative approaches".

---

[9] *Lines 21 to 30 (pag 7). Here I have some doubts about the authors' approach. If the objective is to do a seasonal analysis, the approach is easier than the used by authors. Essentially will be to split each original time series into N series, where N is the number of seasons to be used in the analysis (2, 3, 4) and, then, to apply GEV (as it was previously done with the total time-series) to each seasonal-representative annual maxima Ru time series. Of course, if authors want to use nearshore data, offshore conditions need to be propagated towards the coast. So with this, direction is implicit to the analysis since each seasonal data set will only include waves corresponding to such season, and if there is any directional preference, this will be reflected in the analysis.*

The original goal of the paper is not to perform a seasonal analysis, but a directional one according to the waves' main incident directions of the local wave climate. Actually, we agree that it would be easier to refer to the annual maxima approach (AM) even when performing the directional analysis; moreover, that would ensure as well a more coherent approach to that used for the omnidirectional vulnerability levels computation. We therefore decided to switch from POT to AM also for the computation of the on-shore vulnerability levels. Moreover, we redefined the boundaries of the directional sectors in order to better group the annual maxima H_s incident directions within every single sector. The new sectors are defined as follows:

- Sector 1: $157.5 - 247.5°N$ corresponding to the sectors of Mezzogiorno and Libeccio winds
- Sector 2: $247.5 - 337.5°N$ corresponding to the sectors of Ponente and Mistral winds

In any case, a directional analysis requires to compute the probabilities according to Eq. (4) as explained in the paper.

If we look at the roses of Fig. 7 in the paper (pag. 10), it can be noticed how the waves are most likely to come from a directional sector according to given periods of the year.

Nevertheless, when looking to the AM data, this trend is no longer evident, event though a less marked seasonality for the waves belonging to Sector 2 can be still appreciated (see figure 2 of the present reply). We therefore agree that speaking of "seasonality" for the AM data may confuse the reader, for that we are reviewing the terms "seasonal" and "seasonality" through the whole manuscript, to make clearer the main focus of the investigation.

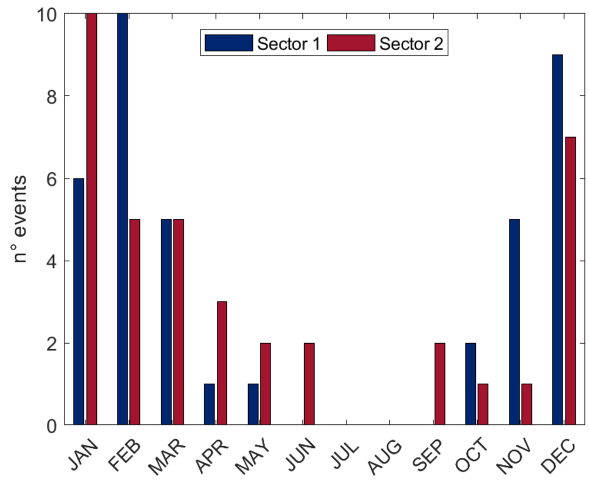

Figure 2: Seasonality of the yearly maxima H_s belonging to the different directional sector.

---

[10] *Line 1 (pag 8). If [9] is applied this is not true, you will obtain N (being N the number of seasons) time series of annual maxima with the same data number than using the total time-series.*

As explained in comment [9], we are performing a directional analysis, and we switched to an AM approach. Then, we are obtained N number of 38 data (being 38 the number of years the hindcast data is defined on), said N the number of directional sector considered.

---

[11] *Lines 2-4 (pag 8). A threshold value of Hs 3 m seems to be high for the area to apply POT. Why authors used this value? How many average storms per year do you obtain? To which percentile of the cumulative distribution is equivalent this value?*

The value of 3m correspond to the 99.2% quantile of the initial H_s distributions. We retained this threshold after performing a sensitivity analysis on the threshold values, given an inter-event duration of 24hours. The value of 3m ensured the resulting dataset to be i.i.d. according to the Kendall's test (Ferguson et al., 2000) and Poisson distributed in frequency due to the Fisher's statistic (Ferguson et al., 2000). Anyway, switching to the AM approach for the directional analysis too, we are no longer commenting on the threshold's selection (thus reviewing all the lines 1-7, pag.8 in the manuscript).

---

[12] *Line 8 (pag. 8). The use of the empirical formula of Callaghan et al (2008) is quite problematic and, probably, not directly applicable. The formula (used coefficients) was obtained with data from a wave buoy in Botany Bay (Australia) where conditions are expected to be substantially different to the one in the study area.*

We definitively agree that the empirical model of Callaghan et al. (2008) has to be tested over the local wave climate conditions. Actually, we selected this formula as, for the strongest sea states of the referring hindcast location, it performs better than the other empirical models commonly encountered in literature (e.g Goda, 2003; Boccotti, 2004, see Fig. 3 of the present reply).

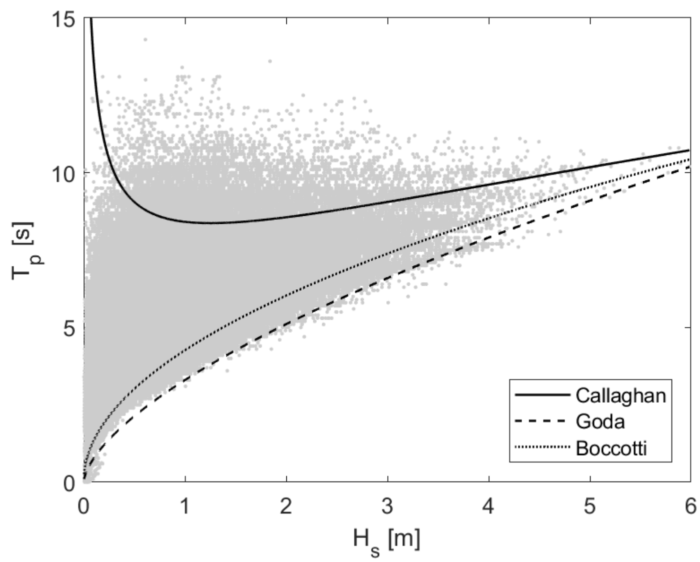

Figure 3: Fitting of different empirical models to the wave height and period of Point_002550.dat dataset.

---

[13] *Lines 14-15 (pag 8). This will depend on the characteristics of the wave climate of the study site (see comment [7]).*

We agree with the referee: "not necessarily" (line 14, pag.8) was actually written to take into account this possibility; in order to enhance this point, we are adding the proposed comment at the end of the line 15, pag. 8. Anyway, looking at the local wave climate, we can reasonably assume that the return periods for wave height and runup lead to very close probability of exceedance (see comment [7]).

---

[14] *Section 3.2 Results presented here cannot formally be named as seasonal analysis but directional analysis. As the text indicates (line 14, pag 10) authors divide wave sin directions and apply EVA to each (directional) dataset.*

As we explained in comment [9], we performed the analysis dividing the incoming wave climate due to two directional patterns. Actually, even when presenting the results of Fig. 9-10-11-12-13 in the paper, we speak of "directional sectors". Nevertheless, as the aforementioned patterns happened to show different seasonal dependences, we considered appropriate to spend a comment on it, even if we did not statistically characterize this link. As previously stated, we reviewed the adopted terminology in order to avoid any misunderstanding.

---

[15] *Pag 11. Results showing T calculated in function of H using eq 5 are not valid (see comment 13). Coefficients of eq 5 have to be derived from local data.*

As we explained in comment [12], although the model of Callaghan et al. (2008) was validated for a different wave climate than that of the area under investigation, we referred to it as it happened to better models the most energetic events. As explained in comment [9], we considered to incorporate the referee's suggestion to adopt an AM approach even for the directional analysis. Thus, we performed again the propagation of waves towards the coast, defining, for each sector at a time, the input wave parameters as follows:

- as regards the significant wave height we selected the data through an AM approach, modelling at a second time through a GEV distribution for the long term parameter estimation;
- regarding the peak period, we are still referring to the model of Callaghan et al. (2008), justifying this choice as explained in [12];
- the incoming direction is still defined according to the approach explained in the paper (Sect. 3.2, pag. 11), with the only difference that the directions are those of the AM events, no longer the POT ones.

---

[16] *Results, Discussion and Conclusions maybe affected by previous comments. Adapt these sections once you decide on them.*

We reviewed Sections 3, 4 and 5 due to the changes done amending reviewer's comments.

---

[17] *Section 5. The comment that using deepwater or nearshore waves give a more reliable CVI assessment is not necessarily true. This will permit to use a wave height more representative of local wave conditions. But, the vulnerability assessment will be more robust or valid provided that CVI properly reflect the conditions of the area. To validate this, you need to compare calculations with reality (e.g. are the vulnerable area usually affected by inundation?).*

We agree that a comparison with historic records would be the key to prove a better vulnerability estimation; unfortunately, as far as we know, this dataset does not exist (or it is not accessible). We spoke of "reliability" as, being the CVI computation closely tied to the incoming wave climate, a proper characterization of it may consequently better detail the vulnerability of the investigated area. This is especially true when the geometry of the bay affects the propagation of the waves towards the shore, as previously noticed in comment [3].

In Section 5, we reviewed lines 18-23 in order to avoid misunderstandings: firstly, on the term "extremes analysis" (as described in comment [2]); secondly, on the use of the term "more reliable", as just explained.

Formal issues

- *Fig [1] Please combine Figs 1 (need to be improved) and 2 (also to be improved) in just one figure.*
  We are removing Fig. 2 as we agreed that it was redundant. We are changing the format of Fig. 1a) to make it clearer.

- *References. Please check them carefully. Some of them are incomplete (e.g. Armaroli and Duo, 2017; Battjes'71), badly cited (De Leo et al. 2017), authors bad included (Bosom and Jiménez 2011; Oscar Ferreira et al. 2017).*
  Amended as suggested.

- *Please check the grammar through the manuscript.*
  Amended as suggested.

References

Boccotti, P. (2004). *Idraulica marittima.* Utet.

Callaghan, D., P. Nielsen, A. Short, and R. Ranasinghe (2008). Statistical simulation of wave climate and extreme beach erosion. *Coastal Engineering 55*(5), 375–390.

Ferguson, T. S., C. Genest, and M. Hallin (2000). Kendall's tau for serial dependence. *Canadian Journal of Statistics 28*(3), 587–604.

Goda, Y. (2003). Revisiting wilson's formulas for simplified wind-wave prediction. *Journal of waterway, port, coastal, and ocean engineering 129*(2), 93–95.

Gornitz, V. M., R. C. Daniels, T. W. White, and K. R. Birdwell (1994). The development of a coastal risk assessment database: vulnerability to sea-level rise in the us southeast. *Journal of Coastal Research*, 327–338.

Kumar, T. S., R. Mahendra, S. Nayak, K. Radhakrishnan, and K. Sahu (2010). Coastal vulnerability assessment for orissa state, east coast of india. *Journal of Coastal Research*, 523–534.

Laudier, N. A., E. B. Thornton, and J. MacMahan (2011). Measured and modeled wave overtopping on a natural beach. *Coastal Engineering 58*(9), 815–825.

McLaughlin, S., J. McKenna, and J. Cooper (2002). Socio-economic data in coastal vulnerability indices: constraints and opportunities. *Journal of Coastal Research 36*(sp1), 487–497.

Plant, N. G. and H. F. Stockdon (2015). How well can wave runup be predicted? comment on laudier et al.(2011) and stockdon et al.(2006). *Coastal Engineering 102*, 44–48.

Sancho-García, A., J. Guillén, G. Simarro, R. Medina, and V. Cánovas (2012). Beach inundation prediction during storms using direferents wave heights as inputs. International Conference on Coastal Engineering.

Stockdon, H., R. Holman, P. Howd, and A. Sallenger Jr. (2006, May). Empirical parameterization of setup, swash, and runup. *Coastal Engineering 53*(7), 573–588.

Stockdon, H. F., D. M. Thompson, N. G. Plant, and J. W. Long (2014). Evaluation of wave runup predictions from numerical and parametric models. *Coastal Engineering 92*, 1–11.

Dear Editor,

we would like to thank the reviewers for their effort in reading and commenting the paper. We went through all the comments and we tried to answer in detail to all of them. An item-by-item reply follows for the Reviewer 2 revisions.

REVIEWER 2

The paper is written clearly and the formulations and methodology are up-to-date, with particular emphasis on the propagation of the wave climate. The figures are of nice quality and results and discussion sections are written clearly. I found the discussion section very enlightening. I only suggest revising the references (i.e. line 7 "Oscar Ferreira").

We thank the Reviewer for his/her interest in our paper and the comments he/she spend on it; as regards the references, we manually fixed the typos present in the paper due to the automatic settings of the Copernicus package, as the referee suggested.

Coastal vulnerability assessment: through regional to local downscaling of wave characteristics along the bay of Lalzit (Albania)

Francesco De Leo[1], Giovanni Besio[1], Guido Zolezzi[2], and Marco Bezzi[2]

[1]Dept. of Civil, Chemical and Environmental Engineering - University of Genoa, Genoa, 16145, Italy
[2]UNESCO Chair in Engineering for Human and Sustainable Development - Dept. of Civil, Environmental and Mechanical Engineering - University of Trento, Trento, 38123, Italy

Correspondence to: Francesco De Leo (francesco.deleo@edu.unige.it)

Abstract.

Coastal vulnerability is evaluated against inundation risk triggered by waves run-up, through the ~~**employment**~~ **evaluation** of ~~**coastal**~~ vulnerability ~~**indexes**~~ **levels** (referred to as ~~**“CVI"**~~ **“VL"**) introduced by Bosom and Jiménez (2011). ~~**CVI**~~ **VL** are assessed through different wave climate characterizations, referring to regional (offshore wave climate) or local (near-shore wave climate) scale. The study is set along the Lalzit bay, a coastal area nearby Durrës (Albania). The analysis reveals that the results vary due to uncertainties inherent in the run-up estimation, showing that the computational procedure should be developed by taking into account detailed information about **the** local wave climate~~**, especially concerning seasonal behaviour and fluctuations**~~**.** Different approaches in choosing wave characteristics for run-up estimation affect significantly the estimate of shoreline vulnerability. The analysis also shows the feasibility and challenges of applying ~~**CVI**~~ **VL** estimates in contexts characterized by limited data availability, through targeted field measurements of the coast geomorphology and an overall understanding of the recent coastal dynamics and related controlling factors.

1 Introduction

Coastal zones are often characterized by a fragile equilibrium, being subjected to hydro-geomorphic processes that change their shape over time and space, and are as well under stress due to the presence of conflicting human activities (Kamphuis, 2010). Moreover, these areas have a huge socio-economic value, which has often triggered their high exploitation in the last decades: coastal population is constantly increasing, together with maritime commerce and coastal tourism (Neumann et al., 2015). This implies enhanced anthropogenic pressures, which challenge their sustainable management and preservation.

The present paper focuses on extreme natural storm events and on their impact on coastal vulnerability within such complex framework. As clearly specified by the Integrated Protocol on Coastal Zone Management (“ICZM"), the effect of storms should be embedded into coastal zone territorial plans and policies, yielding coastal vulnerability assessment (UNEP, 2008). Efficient assessment and decision support tools are required, providing easily accessible information for decision-makers. Coastal vulnerability ~~**Indexes**~~ **assessment** represent**s** a viable option, because ~~**they are**~~ **it is** helpful to classify the shorelines in relation to their vulnerability towards extreme events, such as storms induced inundation and erosion.

~~These indexes~~ **This** usually **requires to** take into account the long term wave statistics and the geomorphology of the beaches to evaluate the level of risk they are exposed to. The estimate of the environmental risk, coupled with the evaluation of the existing anthropic pressure (economic and industrial activities) leads to vulnerability maps. Different approaches to compute ~~CVI~~ **coastal vulnerability** have been so far proposed, which differently combine environmental and socio-economic relevant variables (Gornitz et al., 1994; Soukissian et al., 2010; Di Paola et al., 2014; Fitton et al., 2016; Satta et al., 2016; Ciccarelli et al., 2017; Ferreira et al., 2017; Ferreira Silva et al., 2017; Montreuil et al., 2017; Narra et al., 2017; Mavromatidi et al., 2018, among others). A methodological issue of particular concern is related to the computation of wave climate characteristics suitable for ~~calculating values of the CVI~~ **estimating vulnerability levels** that are of management significance. This can be illustrated by referring to the practical procedure proposed by Bosom and Jiménez (2011) to assess coastal vulnerability to inundation. The procedure foresees to compute the long term run-up values, starting from the ones evaluated through the model of Stockdon et al. (2006) **(hereinafter referred to as S2006)**, and then combining it with the berm or dune heights of a shore to achieve its run-up vulnerability. ~~However,~~ Stockdon et al. (2006) ~~formulation intrinsically leads to a very conservative result, as it provides a value linked to the 2% probability of exceedance: this means that, for given wave and beach characteristic, the computed run-up is not the one most likely occurring, but one of the highest possibly observed within a hypothetical series of records. Therefore, evaluation of high return period run-up values could lead to highly overestimated coastal vulnerability, as the return period is closely tied to the probability of non exceedance. Conversely, the model of~~ Stockdon et al. (2006) ~~has shown to provide more reliable run-up estimates if the input wave parameters are provided in the near-shore region at a depth of 10 m, instead of referring to deep-water values as the original formulation suggests~~ Sancho-García et al. (2012)~~. This requires to change the scale of the wave climate characterization, moving from a national/regional scale to a more detailed local scale in order to obtain reliable estimates for coastal inundation. Such downscaling of the risk analysis implies that wave conditions have to be first propagated towards the shore to evaluate shallow water parameters and afterwards to compute run-up accordingly, leading to more reliable run-up expected value estimate in the case of extreme events~~ (Di Risio et al., 2017)**. However, S2006 formulation intrinsically leads to a conservative result, as it quantifies the run-up exceeded by 2% of the total run-up values induced during a given sea state; this means that, for given wave and beach characteristics, the computed run-up is not the one most likely occurring, but one of the highest possibly observed within a hypothetical series of records. Conversely, if the input wave parameters are provided in the near-shore region at a depth of 10m, S2006 has shown to provide estimates closer to a sea state run-up *expected value* (Sancho-García et al., 2012), also in case of an extreme event (Di Risio et al., 2017). This applies a fortiori when the geometry of the study site is complex (as in the case of the Lalzit bay), thus the wave transformation processes become relevants (Plant and Stockdon, 2015). Such an approach requires therefore to change the scale of the wave climate characterization moving from a national/regional scale to a more detailed local scale.**

The main goal of the present paper is to quantify differences in assessing coastal vulnerability to inundation when using a regional ~~and~~ **rather than** a local (near-shore) characterization of the wave climate~~, and in consideration of its seasonality.~~ **.** The study refers to the bay of Lalzit, immediately north of the city of Durrës (Albania, see Fig. 1). The focus on such rapidly developing context also allows to discuss the potential implications of coastal vulnerability assessment when decision-making requires to be highly adaptive and when data availability is scarce. Preliminary studies on the ~~**characteristic**~~ wave climate characterized ~~**it**~~ **its** ~~**seasonal**~~ directional frames. Building ~~**such**~~ **this** information, it has been possible to compute ~~**seasonal vulnerability indexes**~~ **new vulnerability levels** to be then compared with the offshore omni-directional ones. Such ~~**directional risk**~~ **an** approach is particularly relevant because it could highlight the critical issues related to coastal zone management when the littoral use and exploitation change drastically between different seasons, and represents an additional novelty of the present work.

~~**CVI**~~ **VL** assessment was performed ~~**through the**~~ **Bosom and Jiménez (2011)** ~~**procedure,**~~ referring both to offshore and near-shore wave data, to evaluate variations in shoreline vulnerability depending on the employed spatial (regional/local) and temporal scale (extreme events/seasonal/directional).

The paper is organized as follows: in Sect. 2 we present the indexes computation procedure, along with the investigation area and the data used; in Sect. 3 we show results of coastal vulnerability using wave dataset at regional and near-shore scales; in Sect. 4, results are presented and possible future developments and improvements are discussed.

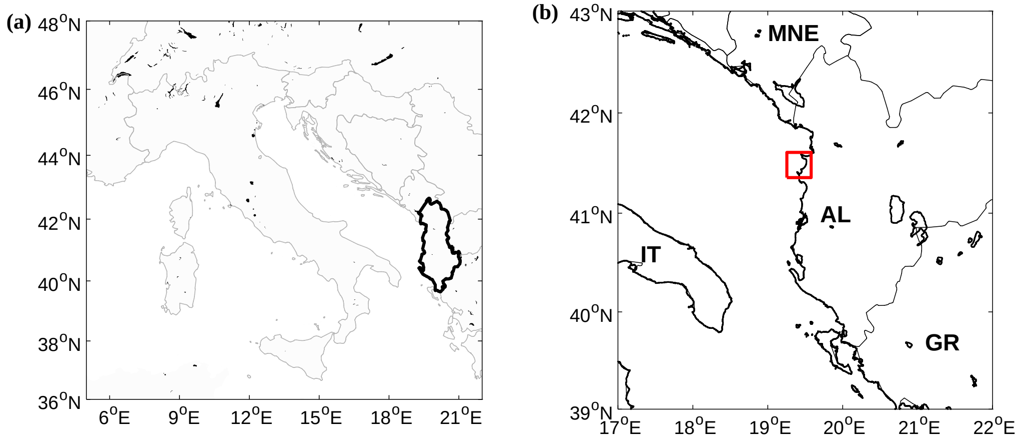

Figure 1. Map showing the area under investigation. a) Location of Albania in South-East Europe and b) the bay of Lalzit underlined within the red frame

2 Data & Methods

The vulnerability assessment is part of a wider research project, aimed at evaluating and quantifying the ongoing coastal erosion affecting the Lalzit bay area. ~~**This phenomenon is due to different causes, concerning the abrupt changes occurred in Albania after the fall of the communist regime that triggered very fast morphological changes either in the watersheds and on the coast**~~ **(De Leo et al., 2017).** In order to collect all the required data, a two weeks field campaign was performed during the month of July 2015.

2.1 Study area: Lalzit Bay, Albania

The Lalzit bay is included between two capes, and can therefore be considered as an independent physiographic unit; it is possible to focus on the processes affecting this coastline independently from those characterizing the nearby physiographic units. A physiographic unit is indeed defined as a portion of shoreline with coherent characteristics in terms of natural coastal processes and of land use, which can thus be studied independently from neighbouring shores (UNEP, 2008). ~~**Specifically, in the Lalzit bay area we identified four main interdependent geophysical and anthropogenic processes that control the dynamics and evolution of the coastal zone (see Fig. ??). The strong interaction among such processes has been identified by**~~ **De Leo et al. (2017)** ~~**as the main mechanism of a massive retreat of the coastline over the past thirty years.**~~

2.2 Field measurements

Field activities were aimed at collecting the minimum required data to investigate the relevant processes affecting **the local** coastal dynamics ~~**presented in Fig. 2**~~. The geomorphology of the beaches along the bay was characterized through sixteen sections ~~**(e.g. Fig. 2)**~~ crossing the shoreline, nearly spaced every kilometre along almost twenty km of the bay length (from sec -4, south, to sec 11, north, see Fig. 3~~**A**~~ **a**). We recorded the cross-shore section elevation at topographically relevant locations, in correspondence of the main slope changes, with particular attention to the submerged bar system. This allowed to assess the cross-shore sections shape, their berm height and the overall cross-shore profile mean slope (**e.g.** Fig. 2). Moreover, we collected different sand samples along every section to characterize their grain size distribution. Sediment samples were taken at selected locations along each section. Every sand sample was analysed through a multi-filter sieve, to assess the weight percentages of sand in each size class, thus building the grading curve. The obtained data were then post-processed by using the software Gradistat (Blott and Pye, 2001), further evaluating the median grain size (d_{50}) for every sampled location. As the resulting values of d_{50} were not significantly varying along each cross-shore profile, we chose to use those characterizing the water edge foreshore as the representative ones of each section.

Results of the grain size surveys are summarized in Fig. 3. The mean grain size (d_{50}) happens to be quite homogeneous among all the sections (Fig. 3~~**B**~~ **b**), and the granulometry of the bay can be considered representative of a "medium sand", according to the classification of Wentworth (1922). The only exception is represented by the section next to the Rodoni cape, which is close to a rocky promontory and is therefore characterized by coarser sediments. On the other hand, cross-shore mean slopes (β_f) and berm heights (B_h) are more variable along the coast, with steeper sections being characterized by lower berms and vice-versa (Fig. 3~~**C, D**~~ **c, d**).

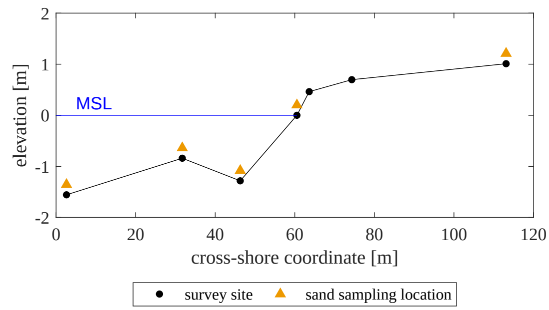

Figure 2. Typical cross-shore profile along the Lazlit Bay (example of section 2, see Fig. 3~~A~~ **a**). It is possible to note the presence of the submerged bar some tens of meters away from the coastline

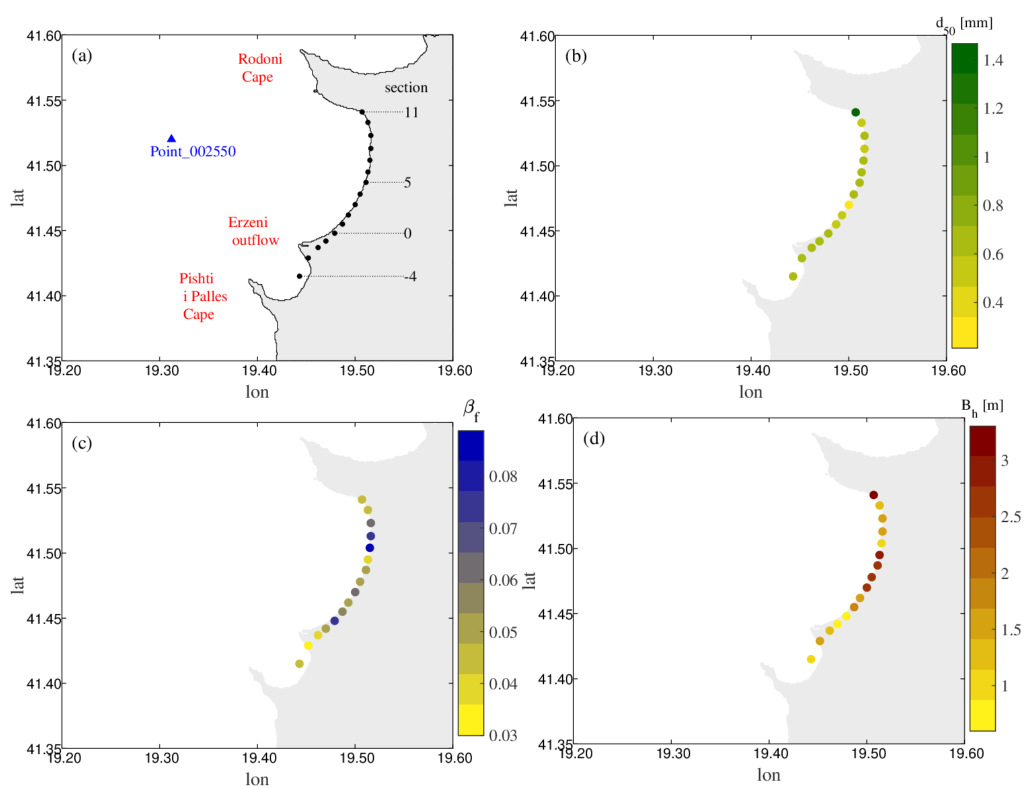

Figure 3. ~~A)~~ **a)** Sampling locations for beach sections (from -4 to 11, from south to north), Point_002550 represents DICCA wave hindcast. Spatially distributed values of: ~~B)~~ **b)** Median grain size (d_{50}); ~~C)~~ **c)** Cross-shore mean slope (β_f); ~~D)~~ **d)** Berm height (B_h)

2.3 ~~Coastal Vulnerability Indexes (CVI)~~ **Vulnerability levels assessment (VL)**

~~CVI~~ **Run-up vulnerability levels** are meant to quantify the vulnerability of a coast toward extreme inundation events. **VL assessment follows the approach proposed by Bosom and Jiménez (2011):** for the investigated beach section (or length of shore), a long term statistical computation for the run-up is required, leading to an intermediate dimensionless variable IV ("Inundation Vulnerability"), defined as follows:

$$IV = \frac{Ru_{2\%}}{B_h} \tag{1}$$

where B_h and $Ru_{2\%}$ are the beach berm or dune height and the long term run-up respectively. For each section, the IV value is then evaluated within a given range, obtained by setting two boundary values:

$$\begin{cases} IV_{min} = \dfrac{Ru_{2\%}}{2Ru_{2\%}} \qquad \Rightarrow Ru_{2\%} = 0.5\ B_h \\ \\ IV_{max} = \dfrac{Ru_{2\%}}{Ru_{2\%} - 2} \qquad \Rightarrow Ru_{2\%} = 2 + B_h \end{cases} \tag{2}$$

It can be noticed that the minimum and the maximum ~~vulnerability levels~~ **values of IV** have a clear physical meaning~~, being explanatory of the cases where the run-up is either half (IV$_{min}$) or two meters higher (IV_{max}) than the berm height.~~ **: actually, IV$_{min}$ is explanatory of the case where the run-up is half of the berm height, ensuring the beach would not be overtopped and thus guaranteeing the protection of the hinterland. On the other hand, IV$_{max}$ refers to a situation characterized by a run-up two meters higher than the berm height and therefore potentially able to flood the hinterland over a substantial area.**

This interval is then scaled to a range from 0 to 1, grouped in five classes of equally spaced vulnerability levels ("very low", "low", "medium", "high", "very high") as reported in Table 1.

IV	0 - 0.2	0.2 - 0.4	0.4 - 0.6	0.6 - 0.8	0.8 - 1.0
VL	very low	low	medium	high	very high

Table 1. Vulnerability levels assessment due to the IV variable

2.4 Wave data and run-up

The assessment of ~~CVI~~ **VL** first requires to compute the long term run-up statistics. Regardless the reference model, run-up computation always implies to combine informations about both characteristic wave climate and morphology of a shore (Battjes, 1971; Holman, 1986; Mase, 1989, among others). As regards the wave data, we referred to the hindcast provided by the Department of Civil, Chemical and Environmental Engineering of the University of Genoa ("DICCA", dicca.unige.it/meteocean/hindcast). The hindcast is defined all over the Mediterranean sea from 1979 to 2016 with a 0.1° resolution both in longitude and latitude, one hourly sampled, and it is based on NCEP Climate Forecast System Reanalysis ("CFSR"), for the period from January

1979 to December 2010 and CFSv2 for the period from January 2011 to December 2016 (Mentaschi et al., 2013). The DICCA hindcast was widely validated (Mentaschi et al., 2015), and, being densely defined over a large time period, it helps to perform reliable long-term statistical computations (Coles and Pericchi, 2003). The location we referred to for this study is shown in Fig. 3a) (Point_002550), whereas data about the shore geomorphology were collected as explained in Sect. 2.2.

Run-up is therefore computed according to **Stockdon et al. (2006)** ~~**model**~~ **S2006** as follows:

$$Ru_{2\%} = 1.1\left\{0.35\,\beta_f\,\sqrt{H_0L_0} + \frac{\left[H_0L_0\left(0.563\,\beta_f^2+0.004\right)\right]^{0.5}}{2}\right\} \tag{3}$$

where β_f stands for the mean slope of the beach, H_0 and L_0 refer to deep water wave height and length respectively.

2.5 Extreme Value Analysis (EVA)

When dealing with run-up estimation, if the data linked to the shore characteristics can be well defined, more uncertainties grow up when trying to empirically parametrize exceptional phenomena (extreme events), of which run-up can be considered as an instance. For this reason we tested two different approaches for the estimation of extreme run-up values.

First, in the frame of a regional analysis, we considered the deep-water data as defined in Point_002550, selecting the annual maxima sea storms from the wave dataset and evaluating the annual maxima run-ups through Eq. (3). This resulted in a 38 extreme run-up dataset for each of the sixteen sections. Every dataset was then modelled through a GEV distribution (Coles et al., 2001), in order to carry out the long term design of run-up values~~**; the validity of the distribution was always proved through the Kolmogorov-Smirnov and the Anderson-Darling parametric tests for every dataset**~~ **(Massey Jr, 1951; Anderson and Darling, 1954)**. Given the distributions, we set two target return periods, literally 50yr and ~~**200**~~ **500**yr, and further computed the resulting run-ups for every section in both cases. This allowed to quantify how ~~**CVI**~~ **VL** estimation could be affected by differently conservative approaches.

Afterwards, we switched from a regional to a locale scale: in this case, EVA were performed directly over the extreme sea storms wave parameters, to assess the 50yr and the ~~**200**~~**500**yr waves. We thus propagated the target waves in front of each section, computing afterwards the long term run-up values. Here, as the wave climate shows ~~**a clear seasonal dependence**~~ **different patterns** with respect to the average incident waves direction, we split the initial wave dataset according to two meaningful directional fetches. This choice involved ~~**two important consequences:**~~ **an important consequence:** ~~**First,**~~ when performing **the** directional analysis, referring return periods for each of the identified sectors have **in fact** to be carefully assigned~~**, as demonstrated by**~~ **Forristall (2004)** **(Forristall, 2004)**:

$$\begin{cases} F_o = \prod_1^N F_i \\ 1 - \dfrac{1}{\lambda_o T_{R_o}} = \prod_1^{N_p}\left(1-\dfrac{1}{\lambda_i T_{R_i}}\right) \end{cases} \tag{4}$$

$$\begin{cases} F_o = \prod_1^{N_p} F_i \\ F = 1 - \dfrac{1}{T_R} \end{cases} \qquad (5)$$

being F the probability of non exceedance, ~~λ **the yearly number of extreme events**~~, T_R the significant return period **and N_p the number of directional patterns**; subscripts o and i stand for omnidirectional and the i^{-th} directional pattern, respectively. The F_i probabilities are fixed in order to obtain N_p equal values whose product gives F_o **(given the referring omni-directional return period)**. ~~**This precaution is due to the fact that, when referring to an omnidirectional analysis, a higher number of events is expected compared to the case of a directional analysis, thus a higher probability of non exceedance (see Eq. (5)). Multiplying the probabilities related to the identified sectors ensures a coherent computational procedure; we therefore previously fixed the referring non-exceedance probability for each sector, in order to get an overall value equal to that of the omnidirectional analysis (given the referring T_{R_o}). Moreover, referring to a subset of the whole dataset implies a lower amount of data to deal with. In order to overcome this drawback, we used the Peaks Over Threshold (POT) approach to come up with long term wave height estimates, imposing a threshold value of 3m and a minimum inter-event duration of 24hr; threshold values were set to get datasets characterized by events being independents and identically distributed, as specified by**~~ **Lang et al. (1999).**

~~**Probabilities**~~ **Then, probabilities** obtained with Eq. (5) ~~**lead to**~~ **were retained to carry out** the long term significant wave heights~~**; in this case we adopted a Weibull distribution applied to the exceedances of the given threshold, as specified in**~~ **DNV (2010)**~~**, testing as well the suitability of the distribution as performed**~~ **, as previously explained for the design run-up values** for the regional analysis. **In both the cases, the validity of the distribution was tested through the Kolmogorov-Smirnov test (Massey Jr, 1951)**.

To completely characterize the target waves (to be downscaled at a later time in the near-shore zone), we linked the peak periods to the computed long term significant wave heights according to the empirical formula of Callaghan et al. (2008). **It should be pointed out that this formula was developed and validated over different wave climates than the one characterizing the investigated area; nevertheless, we decided to rely on it as, for the strongest sea states of the referring hindcast location, it happened to perform better than other empirical models commonly encountered in literature (Goda, 2003; Boccotti, 2004)**~~**; the mean directions**~~ **. As regards the waves mean incident directions, they** were assessed ~~**instead**~~ due to the particular waves climate of the area. Resulting values were set as inputs to the SWAN model (Booij et al., 2003), allowing to get the parameters at a depth of ten meters in front of each of the investigated sections. The obtained wave parameters were then used to compute the 10m depth run-up for both the considered return periods. As regards the bathymetry of the bay, we referred both to the ETOPO1 dataset (www.ngdc.noaa.gov) and a nautical chart of the Italian Hydrographic Institute (www.marina.difesa.it).

It is worth mentioning that the return period of a forcing variate is not necessarily equal to the return period of the outcomes **(Hawkes et al., 2002); .** As an instance, a given return period wave may not lead to the corresponding return period run-up ~~.~~

~~Anyway,~~ **Garrity et al. (2007)** ~~previously~~ **(Hawkes et al., 2002, , in this case it depends on the characteristics of the wave climate of the study site). Nevertheless, when performing the regional analysis, the run-up long term curves computed starting from the annual maxima H_s (say "AM1" approach) happened to lye very close to those linked to the annual maxima retained from the computed initial distribution of run-ups. Furthermore, previous studies** demonstrated that this approach can still lead to satisfactory results **(Garrity et al., 2007)**, and it has already been adopted within ~~previous studies~~ **similar works** (Vitousek et al., 2008). **We therefore decided to refer to the AM1 approach both for the regional and the local scale (omni-directional and directional analysis respectively), as in the latter case it allows to considerably reduce the computational time and effort (there is no need to downscale the whole wave dataset in the shallow waters, but just the target waves).**

3 Results

Once we computed the long term run-ups, we evaluated the resulting ~~CVI~~ **VL** according to the morphology of the testing locations. Since results are punctual (e.g. one index for each of the sixteen sampling locations), we linearly interpolated the ~~CVI~~ **VL** values within hypothetical intermediate sections, in order to get a more meaningful overview about the whole bay.

We initially referred to the regional scale; in this case, an omnidirectional analysis was performed, leading to two sets of results linked to the tested return periods. Secondly, we detailed our study to the local scale: in this case, we got two sets of results for every directional sector taken into account. We first present the ~~CVI~~ **VL** obtained from the regional study.

3.1 Regional scale (offshore wave conditions)

At the regional scale the environmental inputs were the same for each section, being the wave characteristics defined in deep water (Point_002550, Fig. 3~~A~~**a**); the differences in the run-up significant values were just due to different morphological characteristics of each cross-shore section (literally, the mean slope of the different beach profiles). This can be clearly noticed in Fig. 4: the empirical run-ups show the same distribution for every section, as their values are just rigidly translated of a quantity that depends on the value of the section slope β_f (see Eq. 3). From the curves in Fig. 4, the run-ups linked to 50 and ~~200~~**500**yr return period were extrapolated, and the inundation vulnerability ~~indexes~~ **levels** were accordingly computed, as explained in section 2.3. Results are shown in Fig. 5.

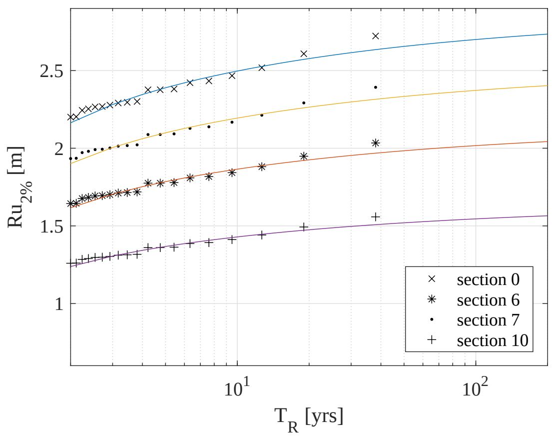

Figure 4. Return period curves for the run-up parameter; results are presented for just some of the cross-sections for the sake of clarity

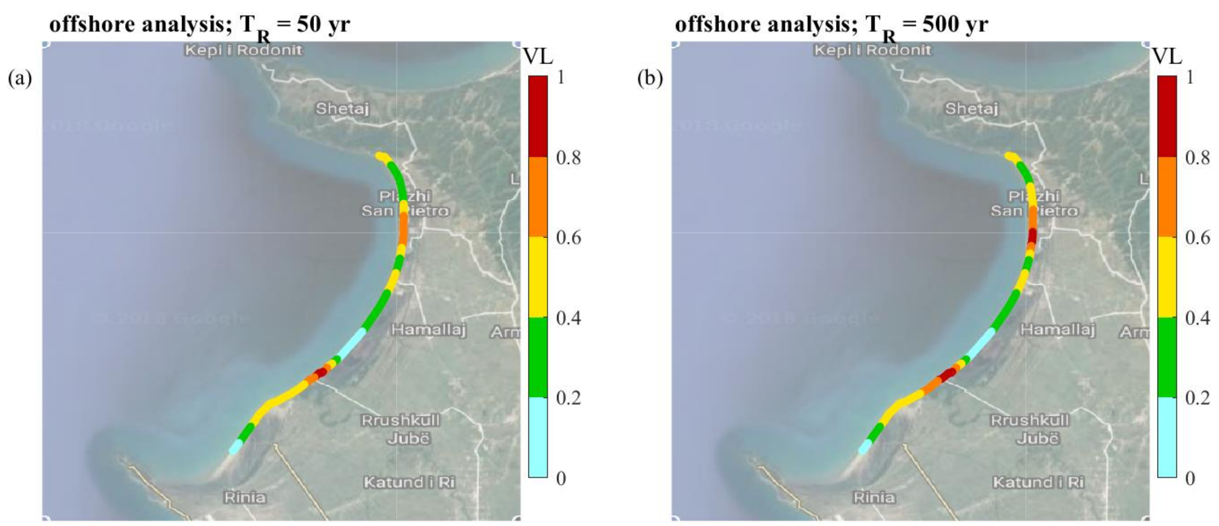

Figure 5. Run-up vulnerability ~~indexes~~ levels for the Lalzit Bay from the regional analysis, using deep water data: a) 50yr return period; b) ~~200~~500yr return period

3.2 Local scale (nearshore wave conditions)

Evaluation of coastal vulnerability ~~indexes~~ **levels** has been carried out also by employing the propagated values of the wave climate at the local scale. It has to be remarked that, in this case, the mean cross-shore slope is not the only changing parameter between one section and another: as waves are propagated toward the shore in front of each of the investigated locations, they are modified due to the occurring transformation processes, resulting in different wave characteristics (heights, lengths and incident directions) depending on the position of a section along the bay.

The first step to compute ~~the indexes~~ **VL** at a local scale is to characterize the wave climate. We mainly referred to the significant wave height, looking at the distribution of the waves prevalent incoming direction ~~over different seasons~~. As shown in Fig. 6~~A)~~**a**), the ~~wave climate of the Lalzit bay is characterized by a strong seasonal behaviour: during the summer months, the prevalent incoming direction happens to be W-NW, whereas for the other seasons waves mainly come from the S-SW direction. We therefore considered two directional sectors, 250-350°N and 190-250°N, being representative of summer and of the rest of the year, respectively.~~ **bay is characterized by waves prevalently propagating from the S-SW and W-NW directions. We therefore considered two directional sectors, literally the third (180-270°N, called 1^{st} sector) and fourth (270-360°N, called 2^{nd} sector) quadrant of the wave rose. Furthermore, it has been previously shown as the waves incoming direction is tied to the seasonality of the wave climate (De Leo et al., 2017), with S-SW being the prevalent incoming direction for waves generated during winter and autumn. This is still reflecting on the annual maxima wave heights, with those belonging to the second sector more uniformly distributed along the year (even though with the peak of occurrence still happening during winter, see Fig. 6b).**

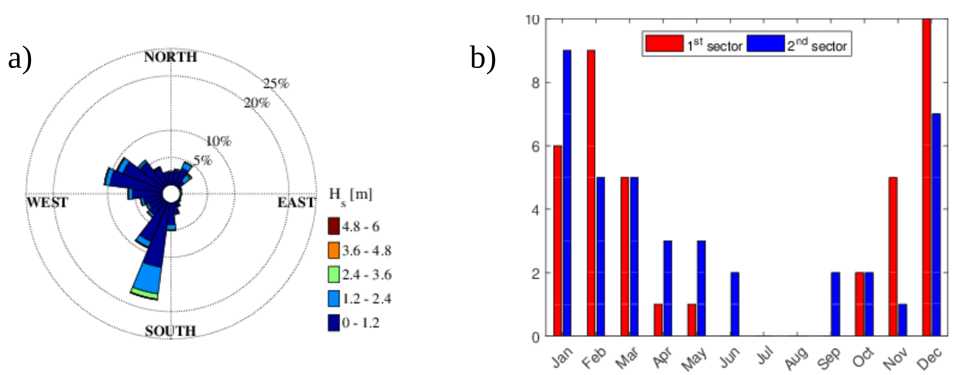

Figure 6. a) Rose of significant wave height for hindcast Point_002550; b) seasonal distribution of the annual maxima wave height due to the considered sectors

Extreme events have been defined for each of the identified sectors, computing the resulting 50yr and ~~200~~**500**yr return period wave heights. The target wave incoming direction for each sector was defined through a linear interpolation, in order to minimize the root mean square error with respect to the directions of the **AM** sea storms ~~identified with the POT approach~~ (see Fig. 7). Finally, for the wave periods, we referred to the empirical equation of Callaghan et al. (2008):

$$\begin{cases} E(T_p) = aH_s^b + cfH_s^{d+g} \\ a = 3.005; b = 0.543; c = 4.82; d = -0.332; f = 1.122; g = -0.039 \end{cases} \tag{6}$$

where H is the target wave height computed through the ~~POT approach~~ **EVA** as previously explained; a, b, c, f, d and g are given parameters.

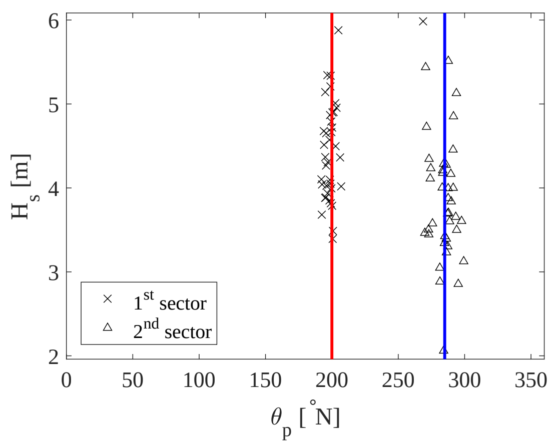

Figure 7. Directions of the extremes waves ~~extracted through the Peaks Over Threshold procedure~~ **belonging to the two considered sectors**

We therefore characterized the design wave for each of the identified directional sectors (W-NW and S-SW), defining its significant height, peak period and angle of attack. These parameters were set at a time as inputs of the wave propagation model, in order to get the shallow water wave parameters. The starting values are shown in Table 3. The inundation vulnerability ~~indexes~~ **levels** following the downscaled wave features are shown in Fig. 8 and 9.

sector [°N]	T_R [yrs]	H_s [m]	T_p [s]	θ_p [°N]
190-250	50	6.49	11.0	200
	200	7.01	11.3	200
250-350	50	6.64	11.1	285
	200	7.17	11.4	285

Table 2. ~~**Design wave parameters for the seasonal directional sectors. Notations T_R is the return period, H_S, T_P, and θ_P stand for wave height, period and incoming direction, respectively.**~~

sector	T_R [yrs]	H_s [m]	T_p [s]	θ_p [°N]
1^{st}	50	6.3	10.9	200.3
	500	7.0	11.3	200.3
2^{nd}	50	5.6	10.5	284.8
	500	6.0	10.8	284.8

Table 3. Design wave parameters for the directional sectors. Notations T_R is the return period, H_S, T_P, and θ_P stand for wave height, period and incoming direction, respectively.

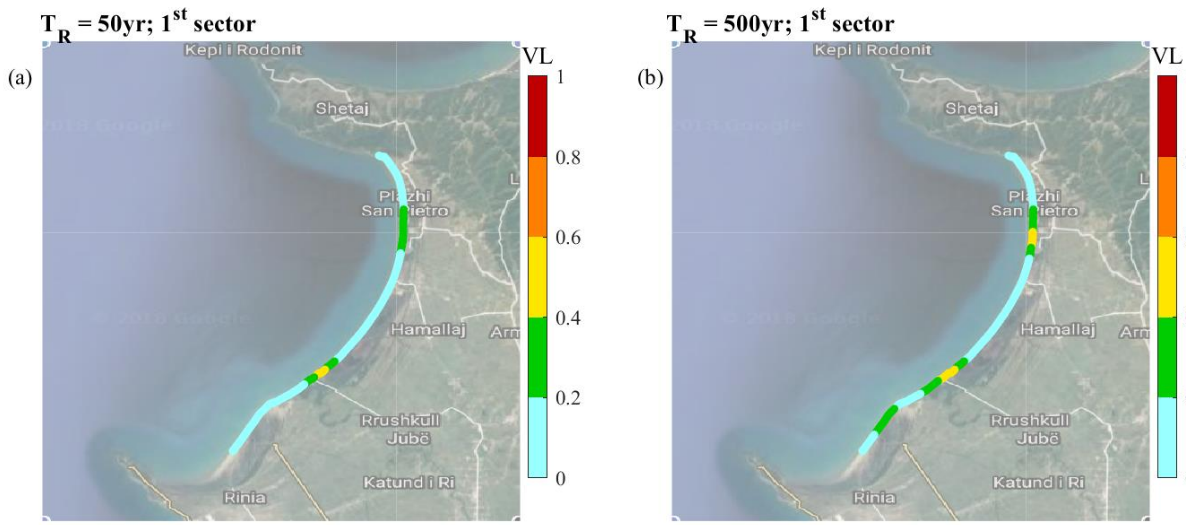

Figure 8. Run-up vulnerability levels for the Lalzit bay, using near-shore data for the 180-270°N sector: a) 50yr return period; b) 500yr return period

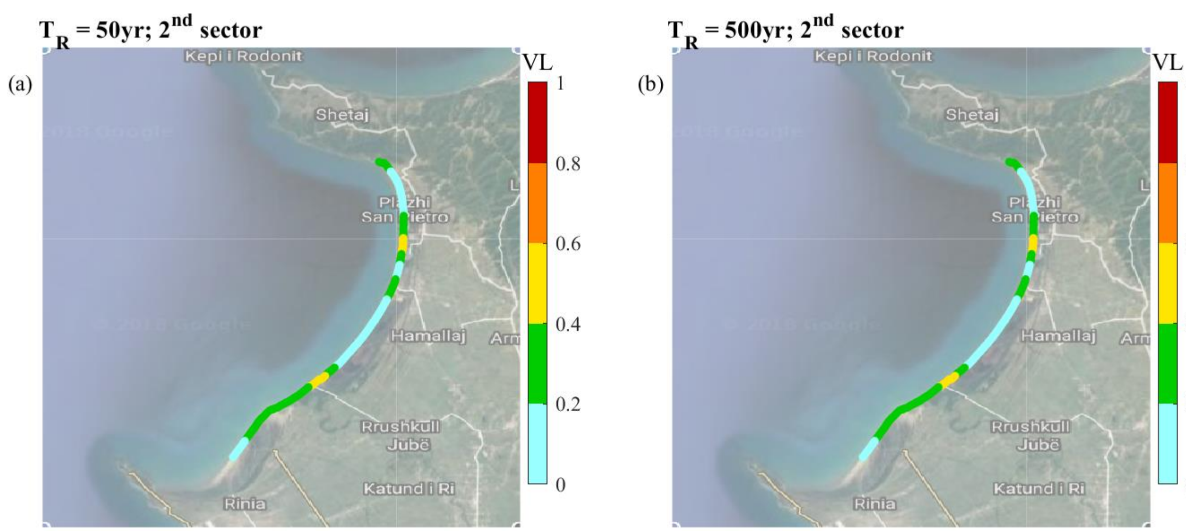

Figure 9. Run-up vulnerability levels for the Lalzit bay, using near-shore data for the 270-360°N sector: a) 50yr return period; b) 500yr return period

For the sake of clarity, in order to compare the results obtained with the two different approaches mentioned before, we discuss just the results linked to the punctual investigated sections; analogous considerations can be therefore extended to the intermediate sections, whose vulnerability levels were assessed through a linear interpolation as previously explained.

Looking at the punctual results (Fig. 10 and 11), it can be noticed that in all considered cases even sections lying next to each other can show very different vulnerability levels: as the sampling locations are $1\mathrm{km}$ distant one from another, their morphological characteristics can significantly vary, and this is consequently reflected in the results.

Referring to the regional scale-offshore analysis and $50\mathrm{yr}$ return period, the vulnerability towards inundation happens to be “very high" in section 0, and still “high" in sections 7, 8; sections -4, 1, 2 are characterized by a “very low" vulnerability, whereas sections 3, 4, 6, 9 and 10 show “low" vulnerability; the other ones are characterized by a “medium" vulnerability. As we could expect, vulnerability levels increase when referring to ~~**200**~~**500**yr return period: in this case, a “very high" vulnerability characterizes section 7 as well, whereas the level increase from “medium" to “high" in section -1, and from “low" to “medium" in section 9; vulnerability class does not change for sections -4, -3, -2, and for sections between 0 and 6.

The directional analysis indicates that results are less varying with respect to the return period: if we refer to the ~~**190-250°N**~~ **1st directional** sector **(180-270°N)**, $50\mathrm{yr}$ return period, vulnerability levels are “very low" for all sections but 7 and 8, which show “low" vulnerability, and 0 (“medium vulnerability"). Switching to the ~~**200**~~**500**yr return period, vulnerability rises from “very low" to “low" in sections -3, -1 **and from “low" to “medium" in section 7**, being unvaried in all the other ones. Results are slightly different for the ~~**250-350°N**~~ **2nd (270-360°N)** sector: in this case, $50\mathrm{yr}$ vulnerability is “low" (instead of “very low") for sections -3, -2, -1, 5, 11; section 7 shows a “medium" instead of a “low" vulnerability. ~~**Again, results proportionally increase due to the considered return period: differences between the previous directional sector can be noted in section -2, 5, 11, being characterized by a “low" vulnerability rather than by a “very low" one; sections 0 and 7 are respectively “high" and “medium" vulnerable, whereas they are characterized by a one step lower vulnerability levels compared to S-SW fetch.**~~ **Here, increasing the return period up to 500yr does not involve any variation in the resultants VL.**

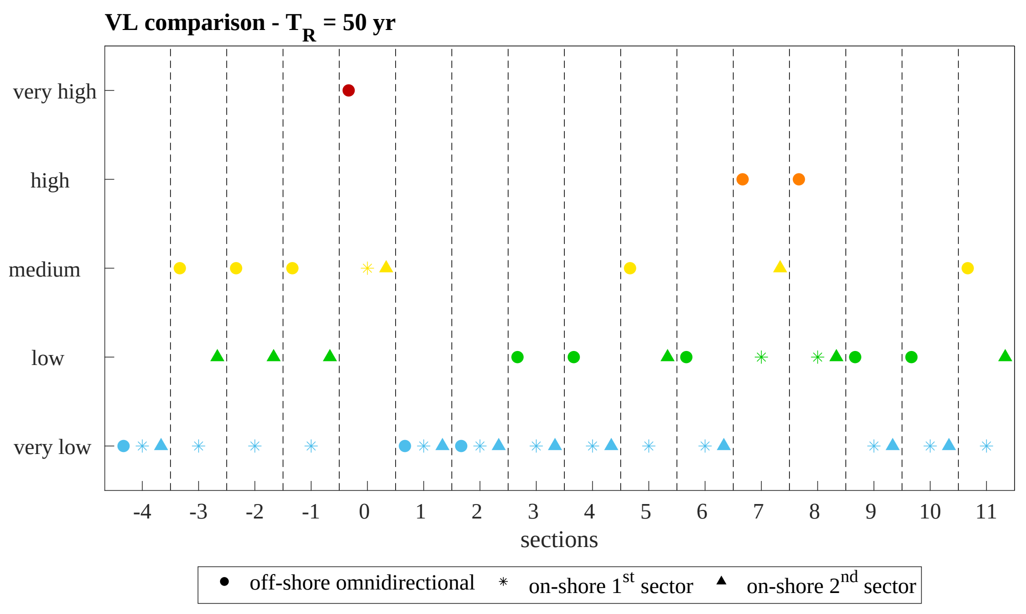

Figure 10. Comparison between the run-up vulnerability indexes for each sampling location; return period equal to 50yr

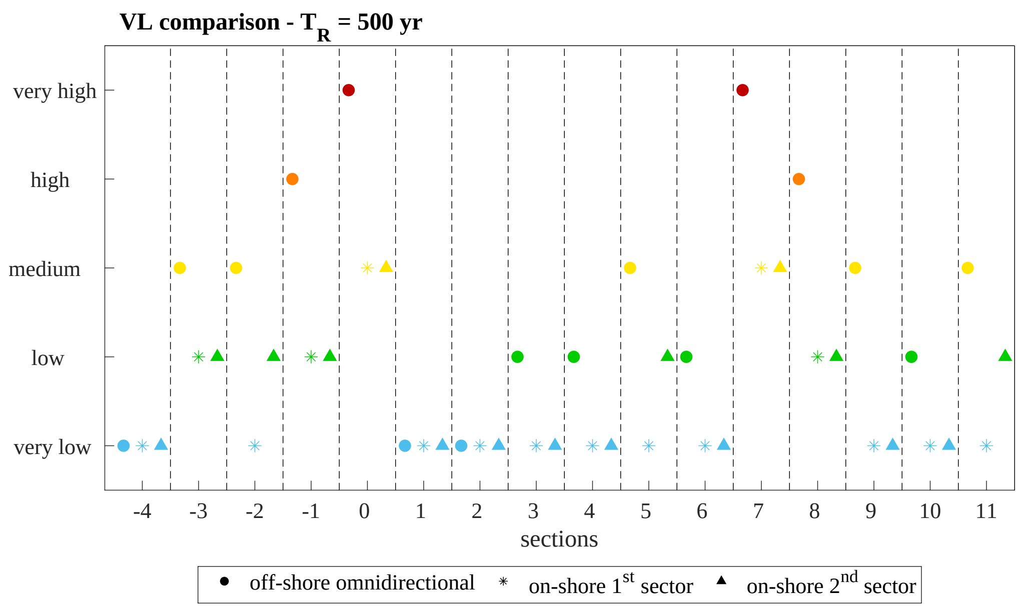

Figure 11. Comparison between the run-up vulnerability indexes for each sampling location; return period equal to ~~200~~500yr

It is interesting to evaluate how VL can change due to the starting wave features: the extreme value analysis performed using deep-water data yields higher vulnerability levels than those obtained after propagating waves toward the shore. Referring to 50yr return period, the most exposed sections are yet characterized by “very high" (0) and “high" (7, 8) levels of vulnerability, whereas ~~is just considering the 200yr return period that the directional analysis lead to a “high" level (section 0, 250-350°N sector); in this case, through omnidirectional analysis sections 7 and -1 become “very high" and “high" vulnerable respectively, whereas the directional analysis carries vulnerability levels never higher than “medium" but that of section 0, precisely.~~ **through the directional analysis vulnerability levels never happen to be higher than “medium", despite the considered return period; to increase from 50yr to 500yr involve at most to move from a “low" to one step higher vulnerability level (section 7, 1st sector), precisely.**

Actually, results divergence decreases for sections characterized by **a** ~~“low" and~~ “very low" vulnerability level~~s~~ **in the northern part of the bay**: in this case, the morphology of the surrounding beach seems to guarantee safe conditions, regardless to the magnitude of the forcing wave.

4 Discussion

As a general trend, assessing coastal vulnerability to inundation using the wave climate computed at the local scale leads to lower vulnerability levels compared to those obtained through the regional analysis. If the vulnerability levels are similarly distributed along the bay (depending on the single section profiles), the long term run-up estimates are clearly dependent to the referring spatial scale: the geometry of the bay indeed strongly affects the waves' propagation toward the coast. Moving onshore, wave heights likely decrease due to refraction and diffraction, which can be expected to be the dominant processes as suggested by the concave enclosed shape of the coast. Consequently, run-up estimates come to be lower when dealing with the local-scale analysis, and resulting ~~CVI~~ **VL** behave accordingly. Results reported in Fig. 10 and 11 highlight another important aspect: if we refer to the local scale, the vulnerability of the bay as a whole is higher when looking at the **wave climate generally characterizing the** ~~summer months~~ **270-360°N sector** ~~(250-350°N)~~. This outcome is justified as well by the geometry of the bay, in fact, even if the starting wave features ~~for the different directional frames are similar~~ **representatives of the third quadrant are higher** (Table 3), waves coming from W-NW are not diffracted by the southern cape as it happens instead for those coming from S-SW. The absence of obstacles along the waves path **(but that of the submerged bar)** implies a lower reduction of the wave heights, involving in turn higher values of the following run-up, thus higher values for the IV variables ~~(see Fig. 12a, b).~~ **Nevertheless, differences between the long term wave parameters due to the considered return period are less pronounced than those of the 1st sector. This is still reflecting on the final run-up values, showing a lower variability which consequently reflects in the final vulnerability levels (whose values do not change among the considered return periods, as it happens instead when looking at the 180-270°N sector).**

Higher run-up estimates due to offshore analysis suggest another consideration about the different variability of the results between regional (offshore) and local (onshore) analysis: as previously demonstrated, the directional data result in a more homogeneous vulnerability level along the coastline. This can be simply justified looking at the vulnerability level computation:

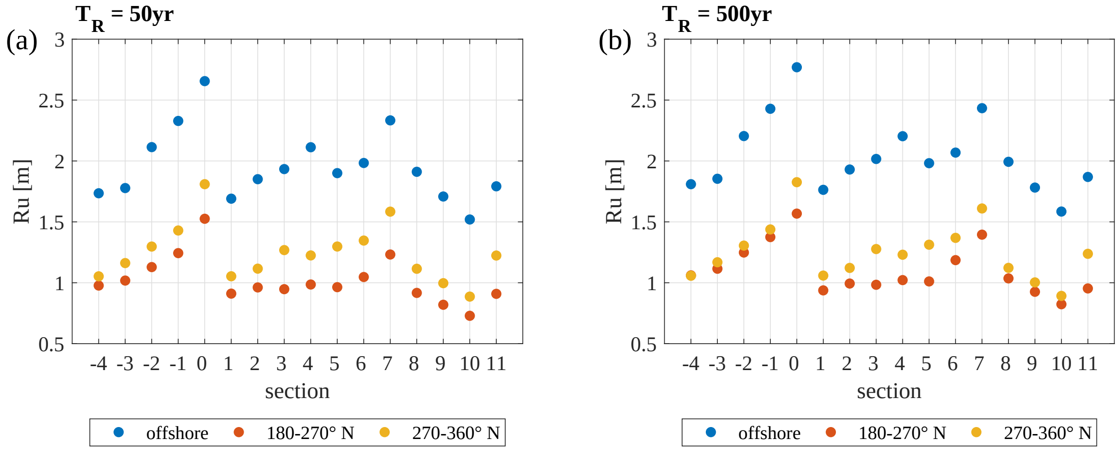

Figure 12. Comparison between run-up values for each section obtained through offshore (regional scale) and near-shore (local scale) conditions: a) 50yr return period; b) ~~200~~**500**yr return period

the same IV index may belong to different vulnerability classes, depending on the value that the IV$_{max}$ variable gets; in fact, while IV$_{min}$ is constant for any of the investigation approaches, the maximum IV depends on the run-up values (see Eq. (2)). High run-up imply lower IV$_{max}$ values, thus a lower total range, which, being spaced in five classes anyway, leads to narrower intervals. Resulting vulnerability levels are therefore more sensitive to smaller variations of the IV values (as Fig. 10 and 11 show).

Finally, if we enlarge our analysis to the coastline as a whole, we can better appreciate how vulnerability is distributed. Despite the differences due to the referring wave data, the most vulnerable areas happen to be those nearby the Erzeni outflow and, in the north, towards the Rodoni cape (see Fig. 3a for references), even if for different causes. If we look at the berm height component, it is evident how the aforementioned areas are characterized by lower berms (Fig. 3d): the Erzeni outflow area has shown in the last years a significant ongoing coastal erosion, as it is estimated that the coastline is retreating at a speed of 0.3$\div$0.5$\mathrm{m/y}$ (Boçi, 1994), resulting in the berms levelling; actually, the concurring reduction of the river sediment transport has also implied steeper profiles (Fig. 3c), that lead to higher run-up estimates. Moving to the north, the lower berms are due instead to the anthropic activities recently developed, which required the levelling of the beach as well; concerning the cross-shore slope, there is actually no evidence of steeper profiles but that of section 7.

5 Conclusions

The vulnerability assessment of a coastline can be a helpful device to plan its land use, as an instance not considering to place high value activities when there's a high risk for the beaches of being submerged or eroded. In this framework, ~~CVI~~ **VL estimates** provide an easy and reliable tool, in order to get an overall overview about a shore vulnerability distribution toward either inundation and/or erosion events.

In this paper, we evaluated the coastal inundation vulnerability for the bay of Lalzit (Durrës, Albania), following the model proposed by Bosom and Jiménez (2011). We first performed a regional analysis, referring to the original formula of Stockdon et al. (2006) **(referred to as S2006)** in order to compute the extreme values for the run-ups at sixteen sections along the bay; then, we detailed the study downscaling the wave features in the shallow waters thanks to a wave propagation model.

We showed that, even if the vulnerability distribution do not change along the shore (e.g. the most exposed sections are placed in the same areas), the results linked to the local scale yield considerably lower vulnerability levels. This is mainly due to the run-up estimates, which are very sensitive to the input wave characteristics, which may be defined in shallow or deep waters. In the case of Lalzit, when waves propagation processes (such as refraction and breaking) become influential, run-up estimates can considerably change depending on the level of detail of wave characterization, as vulnerability levels accordingly do.

Since ~~**the model of**~~ **Stockdon et al. (2006) S2006** ~~**quantifies extreme values**~~ **returns a high statistic** for the run-up variable, it appears more plausible to refer to the modified model as proposed by Sancho-García et al. (2012), to ~~**link it with high return period, without computing extreme analysis twice at a time**~~ **estimate the return period linked to a closer run-up** ***expected value***. This precaution may allow to get ~~**more reliable CVI assessment, properly scaling their related values due to the chosen return period.**~~ **more representative VL assessment, properly scaling their related values due to the chosen return period, particularly when the modifying processes of the waves are relevant.** A critical analysis of the coastline vulnerability could prevent to adopt too much conservative approaches, that could lead to unnecessary countermeasures, translating to loss of money and invasive non required interventions.

The feasibility of ~~**CVI**~~ **VL** assessment can represent a crucial ingredient for rapidly developing and transforming coastal regions such as the Lalzit bay in Albania, which present more options to drive virtuous future coastal development compared to industrialized countries, where ~~**CVI**~~ **coastal vulnerability assessment** may mostly represent a tool for ICZM applied to manage conflicts among relevant stakeholders.

Acknowledgements. This study is part of a project shared between the University of Trento and the University of Genoa (Italy), along with the Polytechnic of Tirana (Albania). The authors would like to thank everyone who joined the field data collection: Alessandro Chesini, Alessandro Dotto, Alessio Maier, Daniele Spada, Dario Guirreri, Erasmo Vella, Federica Pedon, Giorgio Gallerani, Laura Dalla Valle, Martina Costi, Navarro Ferronato, Stefano Gobbi, Tommaso Tosi (University of Trento), Ardit Omeri, Arsela Caka, Bardhe Gjini, Bestar Cekrezi, Erida Beqiri, Ferdinand Fufaj, Idlir Lami, Marie Shyti, Mikel Zhidro, Nelisa Haxhi, Xhon Kraja, Tania Floqi (Tirana Polytechnic). The collected data were then analysed by the Italian partners, in the framework of the UNESCO Chair in Engineering for Human and Sustainable Development (DICAM-Unesco Chair). G. Besio has been funded by University of Genoa through “Fondi per l’Internazionalizzazione" grant.

References

Anderson, T. W. and Darling, D. A.: A test of goodness of fit, Journal of the American statistical association, 49, 765–769, 1954.

Battjes, J. A.: Run-up distributions of waves breaking on slopes, Journal of Waterways and Harbors Division, 97, 91–114, 1971.

Blott, S. J. and Pye, K.: GRADISTAT: a grain size distribution and statistics package for the analysis of unconsolidated sediments, Earth surface processes and Landforms, 26, 1237–1248, 2001.

Boccotti, P.: Idraulica marittima, Utet, 2004.

Boçi, S.: Evoluzione e problematiche ambientali del litorale albanese, Bollettino della Societa Geologica Italiana, 113, 7–14, 1994.

Booij, N., Ris, R., and Holthuijsen, L.: A third-generation wave model for coastal regions, J. Geophys. Res., 104, C4, 2003.

Bosom, G. E. and Jiménez, Q. J. A.: Probabilistic coastal vulnerability assessment to storms at regional scale: application to Catalan beaches (NW Mediterranean), Natural hazards and Earth system sciences, 11, 475–484, 2011.

Callaghan, D., Nielsen, P., Short, A., and Ranasinghe, R.: Statistical simulation of wave climate and extreme beach erosion, Coastal Engineering, 55, 375–390, 2008.

Ciccarelli, D., Pinna, M., Alquini, F., Cogoni, D., Ruocco, M., Bacchetta, G., Sarti, G., and Fenu, G.: Development of a coastal dune vulnerability index for Mediterranean ecosystems: A useful tool for coastal managers?, Estuarine, Coastal and Shelf Science, 187, 84 – 95, 2017.

Coles, S. and Pericchi, L.: Anticipating catastrophes through extreme value modelling, Journal of the Royal Statistical Society: Series C (Applied Statistics), 52, 405–416, 2003.

Coles, S., Bawa, J., Trenner, L., and Dorazio, P.: An introduction to statistical modeling of extreme values, vol. 208, Springer, 2001.

De Leo, F., Besio, G., Zolezzi, G., Bezzi, M., Floqi, T., and Lami, I.: Coastal erosion triggered by political and socio-economical abrupt changes: the cse of Lalzit Bay, Albania, Coastal Engineering Proceedings, 1, 13, 2017.

Di Paola, G., Aucelli, P. P. C., Benassai, G., and Rodríguez, G.: Coastal vulnerability to wave storms of Sele littoral plain (southern Italy), Natural hazards, 71, 1795–1819, 2014.

Di Risio, M., Bruschi, A., Lisi, I., Pesarino, V., and Pasquali, D.: Comparative Analysis of Coastal Flooding Vulnerability and Hazard Assessment at National Scale, Journal of Marine Science and Engineering, 5, 2017.

DNV, D.: C205 Environmental conditions and environmental loads, Recommended Practice, 2010.

Ferreira, O., Plomaritis, T. A., and Costas, S.: Process-based indicators to assess storm induced coastal hazards, Earth-Science Reviews, 173, 159 – 167, 2017.

Ferreira Silva, S., Martinho, M., Capitão, R., Reis, T., Fortes, C., and Ferreira, J.: An index-based method for coastal-flood risk assessment in low-lying areas (Costa de Caparica, Portugal), 114, 90–104, 2017.

Fitton, J. M., Hansom, J. D., and Rennie, A. F.: A national coastal erosion susceptibility model for Scotland, Ocean and Coastal Management, 132, 80 – 89, 2016.

Forristall, G. Z.: On the use of directional wave criteria, Journal of waterway, port, coastal, and ocean engineering, 130, 272–275, 2004.

Garrity, N. J., Battalio, R., Hawkes, P. J., and Roupe, D.: Evaluation of event and response approaches to estimate the 100-year coastal flood for Pacific coast sheltered waters, in: 30th International Conference on Coastal Engineering, ICCE 2006, 3 September 2006 through 8 September 2006, San Diego, CA, United States, pp. 1651–1663, 2007.

Goda, Y.: Revisiting Wilson's formulas for simplified wind-wave prediction, Journal of waterway, port, coastal, and ocean engineering, 129, 93–95, 2003.

Gornitz, V. M., Daniels, R. C., White, T. W., and Birdwell, K. R.: The development of a coastal risk assessment database: vulnerability to sea-level rise in the US Southeast, Journal of Coastal Research, pp. 327–338, 1994.

Hawkes, P. J., Gouldby, B. P., Tawn, J. A., and Owen, M. W.: The joint probability of waves and water levels in coastal engineering design, Journal of hydraulic research, 40, 241–251, 2002.

Holman, R.: Extreme value statistics for wave run-up on a natural beach, Coastal Engineering, 9, 527–544, 1986.

Kamphuis, J. W.: Introduction to coastal engineering and management, vol. 30, World Scientific Publishing Co Inc, 2010.

Lang, M., Ouarda, T., and Bobée, B.: Towards operational guidelines for over-threshold modeling, Journal of hydrology, 225, 103–117, 1999.

Mase, H.: Random Wave Runup Height on Gentle Slope, Journal of Waterway, Port, Coastal, and Ocean Engineering, 115, 649–661, 1989.

Massey Jr, F. J.: The Kolmogorov-Smirnov test for goodness of fit, Journal of the American statistical Association, 46, 68–78, 1951.

Mavromatidi, A., Briche, E., and Claeys, C.: Mapping and analyzing socio-environmental vulnerability to coastal hazards induced by climate change: An application to coastal Mediterranean cities in France, Cities, 72, 189 – 200, 2018.

Mentaschi, L., Besio, G., Cassola, F., and Mazzino, A.: Developing and validating a forecast/hindcast system for the Mediterranean Sea, Journal of Coastal Research, SI 65, 1551–1556, 2013.

Mentaschi, L., Besio, G., Cassola, F., and Mazzino, A.: Performance evaluation of WavewatchIII in the Mediterranean Sea, Ocean Modelling, 90, 82–94, 2015.

Montreuil, A.-L., Chen, M., and Elyahyioui, J.: Assessment of the impacts of storm events for developing an erosion index, Regional Studies in Marine Science, 16, 124 – 130, 2017.

Narra, P., Coelho, C., Sancho, F., and Palalane, J.: CERA: An open-source tool for coastal erosion risk assessment, Ocean and Coastal Management, 142, 1 – 14, 2017.

Neumann, B., Vafeidis, A. T., Zimmermann, J., and Nicholls, R. J.: Future coastal population growth and exposure to sea-level rise and coastal flooding-a global assessment, PloS one, 10, e0118 571, 2015.

Plant, N. G. and Stockdon, H. F.: How well can wave runup be predicted? Comment on Laudier et al.(2011) and Stockdon et al.(2006), Coastal Engineering, 102, 44–48, 2015.

Sancho-García, A., Guillén, J., Simarro, G., Medina, R., and Cánovas, V.: Beach inundation prediction during storms using direferents wave heights as inputs, vol. 1, p. 32, 2012.

Satta, A., Snoussi, M., Puddu, M., Flayou, L., and Hout, R.: An index-based method to assess risks of climate-related hazards in coastal zones: The case of Tetouan, Estuarine, Coastal and Shelf Science, 175, 93–105, 2016.

Soukissian, T. H., Ntoumas, M. C., Anagnostou, C., Kiriakidou, C., et al.: Coastal Vulnerability of Eastern Saronikos Gulf to intense natural events, in: The Twentieth International Offshore and Polar Engineering Conference, International Society of Offshore and Polar Engineers, 2010.

Stockdon, H., Holman, R., Howd, P., and Sallenger Jr., A.: Empirical parameterization of setup, swash, and runup, Coastal Engineering, 53, 573–588, 2006.

UNEP, M.: ICZM Protocol in the Mediterranean, available at: www. pap-thecoastcentre. org, 2008.

Vitousek, S., Fletcher, C. H., and Barbee, M. M.: A practical approach to mapping extreme wave inundation: Consequences of sea-level rise and coastal erosion, in: Solutions to Coastal Disasters 2008, pp. 85–96, 2008.

Wentworth, C. K.: A scale of grade and class terms for clastic sediments, The Journal of Geology, 30, 377–392, 1922.